Biophysical Characterization of an ABC L-methionine Transporter

Thesis by
Qi Wen Li

In Partial Fulfillment of the Requirements for the
degree of
Doctor of Philosophy

CALIFORNIA INSTITUTE OF TECHNOLOGY
Pasadena, California

2017
Defended Jan 12, 2017

Qi Wen Li
ORCID: 0000-0001-9493-2316

ACKNOWLEDGEMENTS

[Intentionally Left Blank]

ABSTRACT

The ATP-binding cassette (ABC) superfamily is pivotal to a number of important biochemical processes and ubiquitous in all kingdoms of life. Previous studies of ABC transporters have been heavily focused on the structural determination of the different intermediates of the transport cycle. In order to characterize the mechanism of an *E. coli* L-methionine transporter, which is an ABC importer, we first collated previously reported structural information on the conformational states of several well characterized ABC importers and associated binding proteins, and identified four major conformations (i.e., pre-T, outward, post-T, and inward state). We stabilized these intermediates using appropriate mutations, substrates, and nucleotides. We then studied the kinetics and thermodynamics of the formation of these states using surface plasmon resonance (BiaCore, GE Healthcare) and MicroScale Thermophoresis (NanoTemper). We developed a quantitative model that details the kinetic and molecular mechanism of *E. coli* MetNI. Towards this goal, we extended the Two-State, alternating access model to include other intermediates that are crucial to transport and are using this to provide a temporal understanding of transport. While this model is developed to describe the behavior of the L-methionine MetNI importer, it may also have predictive power for other ABC Type I importers, since the NBD's response for coupling transport to ATP-binding and hydrolysis are highly conserved in this family.

PUBLISHED CONTENT AND CONTRIBUTIONS

Nguyen, P. T. et al. (2015). "The contribution of methionine to the stability of the Escherichia coli MetNIQ ABC transporter-substrate binding protein complex". In: *Biol Chem* 396.9-10, pp. 1127–34. ISSN: 1437-4315 (Electronic) 1431-6730 (Linking). DOI: 10.1515/hsz-2015-0131. URL: http://www.ncbi.nlm.nih.gov/pubmed/25803078.

Q.W.L performed the MST experiments, prepared the data, and participated in the writing of the manuscript.

TABLE OF CONTENTS

LIST OF ILLUSTRATIONS

Number *Page*

LIST OF TABLES

Chapter 1

INTRODUCTION

Membrane carriers are responsible for moving solutes across biological membranes for purposes that are essential to maintaining cellular homeostasis, including nutrient intake and waste disposal. Their very existence arises from the nearly impermeable nature—with the exception of very small, uncharged molecules like oxygen and nitrogen—of biological membranes. All other transport requires that a membrane-facilitator move substrates in and out of membranes. Passive transport takes advantage of the downhill electrochemical gradient, while active transport requires the coupling of an energy source to enable the thermodynamically unfavorable reaction. The ATP-binding cassette (ABC) transporters are active transporters that couple substrate transport with obtaining energy stored in the high-energy phosphate bonds of adenosine triphosphate (ATP). To accommodate transport needs of cells, many different transporters are encoded in the genomes of organisms. In *E. coli*, about 10% of the genome encodes for transport purposes. One third of the transporters are ABC transporters (Rees, Johnson, and Lewinson, 2009).

1.1 ABC Transporters

ABC transporters are one of the largest transporter families. They belong to a superfamily of integral membrane proteins that power the movement of many different types of solutes across the membrane through energy harvested from ATP binding and hydrolysis.

ABC transporters function either as importers to bring in nutrients (Hollenstein, Frei, and Locher, 2007), or exporters to move out lipids, toxins, and wastes. ABC transporters are present in all kingdoms of life (Linton and Higgins, 1998). While ABC exporters exist in both prokaryotes and eukaryotes, importers are only found in prokaryotes (Linton and Higgins, 1998). There are about 50 ABC transporters found in humans (Dean, Rzhetsky, and Allikmets, 2001; Moitra and Dean, 2011). They are involved in the regulation of ions and solute concentration in many vital biochemical processes, including multidrug resistance (Lage, 2003), cholesterol and lipid transport, and homeostasis (Riordan, 2008; Aittoniemi et al., 2009; Bryan et al., 2007). Malfunction of these proteins in eukaryotes is known to cause several diseases, including cystic fibrosis, diabetes, and hypercholesterolemia (Dean and

Annilo, 2005). These examples underline the necessity for a greater understanding of the mechanistic behavior of ABC transporters.

The architecture of an ABC importer consists minimally of four domains: two transmembrane domains (TMDs) that are located in the lipid bilayer, and two highly conserved nucleotide binding domains (NBDs, or ABCs) with the two bound ATPs sandwiched between the two Walker A motifs. ABCs can be further divided into two subdomains: first, the catalytic core domain, which contains the conserved P-loop or Walker A motif (GXXGXGK(S/T)), and a Walker B motif (xxxxD, x = hydrophobic), a Q-loop and an H-loop (or switch region), and second, a more structurally diverse alpha helical domain, which contains the ABC signature motif LSGGQ. The catalytic core has a Walker A region that is critical for ATP binding and a Walker B region that is essential for hydrolysis. The general structures of ABC transporters can be demonstrated through two structures, BtuCDF (Korkhov, Mireku, and Locher, 2012) and Sav1866 (R. J. Dawson and Locher, 2007). Additional domains that have regulatory functions can be fused to the TMDs or NBDs. Examples include OpuA, MalK, and the cystic fibrosis transmembrane conductance regulator (Rees, Johnson, and Lewinson, 2009; Kadaba et al., 2008; S. Chen et al., 2013).

ABC importers only exist in prokaryotes, therefore, ABC importers are structurally unique to microbes. They represent a unique appeal, such as studying peptidoglycan biosynthesis for the rational design of antibacterial agents. Multiple drug resistance (MDR) transporters are a type of ABC transporter (Lage, 2003). Multidrug resistance is a major challenge in cancer and infectious diseases. Such resistance interferes with treatments and leads to longer recovery times and higher mortality rates (Dean, Rzhetsky, and Allikmets, 2001).

Experiments targeting the structures of ABC transporters during these conformational changes have further illuminated the transport process, particularly the role of NBDs. The NBD consists of a highly conserved catalytic core (Higgins, Hiles, et al., 1986) and a more structurally diverse alpha-helix domain (Schmitt et al., 2003). The spatial location of these two domains is used to classify the state of the NBDs. They have been observed in multiple conformations: open, semi-open, and closed (Kadaba et al., 2008; Oldham and J. Chen, 2011a; Oldham and J. Chen, 2011b). The closed NBD state is when the two domains are packed closely next to each other sandwiching ATP. In contrast, open NBDs occur when the two NBDs move away from the central axis of the transporter. Semi-open NBDs correspond

to the state intermediate between open and closed. The closing of NBDs is believed to be driven by the binding of ATP, while the opening of the NBDs is stimulated by hydrolysis (Moody et al., 2002). The opening and closing of NBDs are connected to multiple events, such as ATP binding and hydrolysis, binding protein association and dissociation, hydrolysis products dissociation, and others (Oldham and J. Chen, 2011a).

The proper function of most ABC importers relies on a periplasmic binding protein to capture substrate and initiate transport. These proteins were first discovered when cells were subjected to osmotic shock and binding proteins were released to the solution (Heppel, 1969), suggesting that they are soluble proteins, which indeed they are. When substrate diffuses to the periplasm, the binding protein binds to it with high enough affinity to sequester substrate, which may be present in low concentration.

The Alternating Access Model

How does a membrane facilitator move a molecule from one side of the membrane to another? An important concept in the ABC transporter mechanistic analysis was introduced in the 1960s, and it has had a strong influence on the field (Jardetzky, 1966), the alternating access model. According to this model, membrane carriers have two major conformations, one opens up towards the periplasm, the other the cytoplasm. They are called the outward-facing and inward-facing conformation, respectively. Several ABC transporter systems have demonstrated to follow this framework. Since the alternating access model is an oversimplification of the transport mechanism, we aim to elucidate a detailed mechanism that explains how conformational changes couple with substrate translocation and ATP hydrolysis to complete the reaction.

1.2 A Methionine ABC Transporter, MetNI

MetNI belongs to the ABC transporter superfamily. It was discovered in the 1970s through a set of elegant *in vivo* experiments (Kadner, 1974). Kadner also identified methionine derivatives, such as D-methionine, that are substrates of MetNI (Kadner, 1977). Importantly, he established that under high intracellular L-methionine concentration, transport is inhibited. This feedback mechanism is known as "trans-inhibition" (Kadner, 1975) and appears to be unique to MetNI.

When a structure of the inward-facing conformation of MetNI was determined (Kadaba et al., 2008), the molecular architecture was available for close examination.

MetNI is an integral membrane protein that consists of two TMDs and two NBDs; each NBD divides into two subdomains, the nucleotide binding site and the C-terminal (C2) regulatory domain. The mechanism of trans-inhibition that Kadner observed was not well understood previous to this paper; the observation that the intracellular L-methionine concentration modulates the rate of transport through a negative feedback loop helped to clarify this. In this 2008 paper, when the MetNI crystal was soaked with selenomethionine, the electron density shows evidence that methionine binds to the C2 domain. This suggests that trans-inhibition is mediated by the C2 domain. It is hypothesized that when the imported substrate builds up in the cytoplasm, L-methionine binds to the C2 domain and results in the inhibition of hydrolysis and transport (Kadner, 1974; Kadner, 1975; Kadner, 1977). Kinetic assays show that L-methionine inhibits hydrolysis non-competitively (Yang and Rees, 2015).

The MetNI system has a 30 kDa binding protein, MetQ. It co-purifies with substrate L-methionine. This indicates the high affinity binding of the substrate to MetQ. This notion was later confirmed with affinity measurement by an SPR assay; it was determined to be around 10 nM. The liganded MetQ has been captured in X-ray crystallography (Nguyen et al., 2015). The observed bond/salt bridge network between protein side chains and the methionine -amino and carboxyl groups is thought to contribute to the high affinity of the ligand binding to MetQ (Nguyen et al., 2015). MetQ consists of two domains: the N- and C-domain. While each lobe has a conserved topology, variations in the connections between the lobes can be used to classify periplasmic binding proteins into distinct clusters (Berntsson et al., 2010). The opening and closing of these two lobes created two major conformations: open and closed (Mao et al., 1982). Unlike the maltose transporter system, MetQ does not seem to partake in the regulation of transport.

1.3 The Overarching Questions

There are many interesting questions concerning the transport mechanism that MetNI employs to efficiently uptake L-methionine. To elucidate this mechanism, we would like to address: (1) How do the rate and affinity constants help to understand the transport mechanism? (2) What are the advantages of having a binding protein? (3) What is the transport mechanism for MetNI? (4) Is this mechanism universal for all ABC transporters? To address these questions, we first set up a kinetic framework and evaluate information given by each model, starting from a simple system.

1.4 Transporter Kinetics

Developing a kinetic mechanism that can accurately account for the behavior of transport proteins is a good way to encapsulate what we learn about membrane carriers and apply the knowledge of one system to another. To approach this, a simplified model is examined to get familiar with the logistics of a transport process under general conditions.

A General Simple Kinetic Transport Model, M1

We start with a model (Dill and Bromberg, 2003) that assumes there are only four states of the carrier during transport. Membrane transport follow four steps: (1) the carrier binds the solute on one side of the membrane; (2) the carrier hauls the solute across; (3) the carrier unloads the solute on the opposite side of the membrane; (4) the carrier resets itself. The goal is to calculate the rate of solute being carried across the membrane based on the energetic difference between the two spaces separated by an impermeable surface. We describe transport going from left to right, but the kinetic mechanism applies to the opposite direction as well.

This model should extend to include the coupling of an energy source. Carriers that are involved in gradient driven transport are called channels, while those involved in active transport are called pumps and transporters. The M1 model is a general description of all carriers, each type of transport is a special case of this model.

The rate of solute across the membrane can be calculated as:

$$V_{\text{transport}} = k_r[\text{ES}_\text{l}] - k_l[\text{ES}_\text{r}] \tag{1.1}$$

The total concentration of enzyme is conserved:

$$[\text{E}_\text{tot}] = [\text{ES}_\text{l}] + [\text{E}_\text{l}] + [\text{ES}_\text{r}] + [\text{E}_\text{r}] \tag{1.2}$$

At steady state, the rate of solute transport must be equal to the rate of the carrier resetting itself:

$$V_{\text{transport}} = V_{\text{reset}} \tag{1.3}$$

The association constants K_l and K_r are defined as follows:

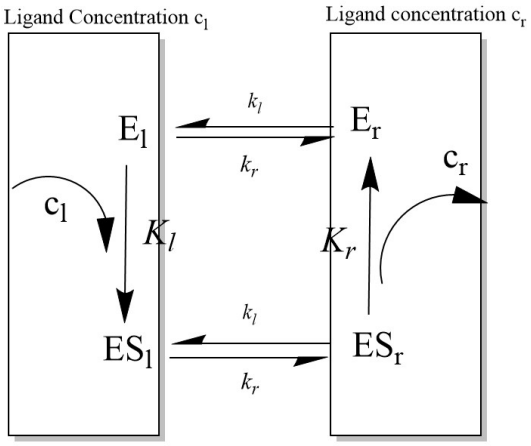

Figure 1.1: **A model of carrier proteins transporting solute across membranes** (Dill and Bromberg, 2003). The scheme starts from the left side of the membrane where the carrier, E_l, binds to solute, c_l, and forms an enzyme-substrate complex, ES_l. This complex changes its conformation to ES_r, which exposes the solute to the right side of the membrane. Then ES_r dissociates and yields E_r and c_r on the right side of the membrane. Finally, the carrier resets itself from E_r to E_l. This model describes a general transport mechanism. Active Transport, which is a special case of this model, extends from the basic scheme.

on the left side:

$$K_l = \frac{[ES_l]}{[E_l][c_l]} \tag{1.4}$$

on the right side:

$$K_r = \frac{[ES_r]}{[E_r][c_r]} \tag{1.5}$$

Combining Equations 1.2 and 1.3, we have:

$$[ES_l] = [E_{tot}](\frac{k_l}{k_r + k_l})(\frac{K_l[c_l]}{K_l[c_l] + 1}) \tag{1.6}$$

Since the system is symmetric, $[ES_r]$ is:

$$[ES_r] = [E_{tot}]\frac{k_r}{k_r + k_l}(\frac{K_r[c_r]}{K_r[c_r] + 1}) \tag{1.7}$$

Solving for $V_{transport}$ yields:

$$V_{transport} = k_r[ES_l] - k_l[ES_r] = [E_{tot}](\frac{k_l k_r}{k_r + k_l})(\frac{K_l[c_l]}{K_l[c_l] + 1} - \frac{K_r[c_r]}{K_r[c_r] + 1}) \tag{1.8}$$

The maximum rate of transport occurs when $(\frac{K_l[c_l]}{K_l[c_l]+1} - \frac{K_r[c_r]}{K_r[c_r]+1})$ equals to 1. Therefore, V_{max} can be expressed as:

$$V_{\max} = [\mathrm{E_{tot}}](\frac{k_r k_l}{k_r + k_l}) \tag{1.9}$$

$V_{\text{transport}}$ can be expressed in terms of $V_{\max}$:

$$V_{\text{transport}} = V_{\max}(\frac{K_l[\mathrm{c_l}]}{K_l[\mathrm{c_l}] + 1} - \frac{K_r[\mathrm{c_r}]}{K_r[\mathrm{c_r}] + 1}) \tag{1.10}$$

Passive Transport, a special case of the model

During passive transport, solute moves from the side of the membrane with higher solute concentration to the other side. In the simplest passive transport case, the affinity for solute on the left is the same as the right. Therefore, we define a general K:

$$K = K_l = K_r \tag{1.11}$$

Let's say the solute is passively moving from the left to the right; then we have

$$[\mathrm{c_l}] > [\mathrm{c_r}] \tag{1.12}$$

For passive transport, when the solute concentration is very low, we have

$$K[\mathrm{c_l}] \ll 1 \tag{1.13}$$

and

$$K[\mathrm{c_r}] \ll 1 \tag{1.14}$$

Under these specific conditions of passive transport, Equation 1.10 can be reduced to the below:

$$V_{\text{transport}} = V_{\max} K([c_l] - [\mathrm{c_r}]) \tag{1.15}$$

That means when the concentration of solute is small and when the affinity of the carrier protein that binds to the substrate from either side of the membrane is equal, the rate of passive transport is linearly proportional to the difference of the concentration on both side, which is the concentration gradient across the membrane.

However, when the concentration of solute is sufficiently high, the flux first rapidly decreases, then the decrease slows down to plateau, then the transport reverses directions, as indicated by a negative flux following Equation 1.10 (Figure. 1.2).

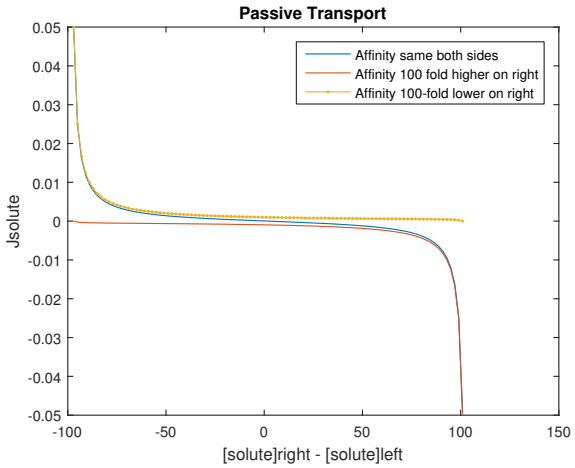

Figure 1.2: **Passive transport when the solute concentration is high.** The rate of solute transported across the membrane is plotted against the ratio of the concentrations of the solute on the right side of the membrane over the left. The equation used for graphing this is Equation 1.15

A Three State Kinetic Model with a Binding Protein, M2

We include additional components for the transporter, a binding protein, Q, and an energy source, ATP (Figure 1.3), to better understand the kinetic mechanism of active transport by ABC importers. Prokaryotic importers depend on high affinity periplasmic binding proteins to transport.

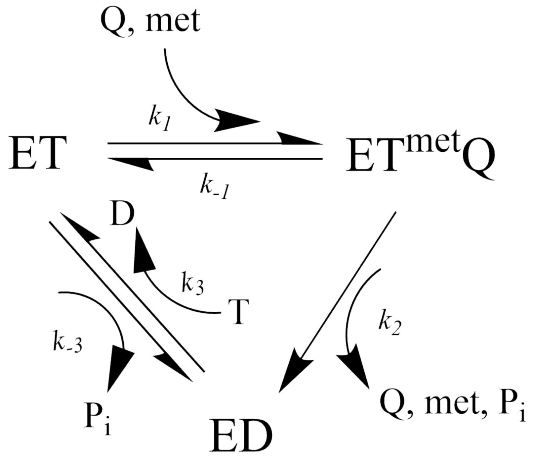

Figure 1.3: **ATP-powered transporter in a binding protein dependent system** This model starts with a transporter bound to ATP (i.e. 'ET'), which binds to substrate (i.e. 'met') and 'Q' to form the enzyme-substrate complex '$ET^{met}Q$'. This complex subsequently hydrolyzes ATP, dissociates 'Q', and delivers methionine to yield ED. To reset the cycle, the ADP in 'ED' is replaced by ATP to form 'ET'.

The steady state rate equation can be derived as follows:

Mass conservation:

$$[\mathrm{E_{tot}}] = [\mathrm{ET}] + [\mathrm{ET^{met}Q}] + [\mathrm{ED}] \tag{1.16}$$

In steady state, the rate of formation of $[\mathrm{ET^{met}Q}]$ equals the rate of consumption of $[\mathrm{ET^{met}Q}]$

$$k_1[\mathrm{ET}][\mathrm{Q}] = (k_{-1} + k_2)[\mathrm{ET^{met}Q}] \tag{1.17}$$

In steady state, the rate of substrate transport must be equal to the rate of the transport resetting itself,

$$k_2[\mathrm{ET^{met}Q}] = k_3[\mathrm{ED}] - k_{-3}[\mathrm{ET}] \tag{1.18}$$

We assume that the ligand binding is at equilibrium where k_{-1} >> other rates, and k_1 [Q] >> other rates, and the dissociation constant K is defined as:

$$K = \frac{k_{-1}}{k_1} \tag{1.19}$$

The rate of transport is,

$$V_{\mathrm{transport}} = \frac{d[\mathrm{met}]}{dt} = k_2[\mathrm{ET^{met}Q}] = \frac{\frac{k_2k_3}{k_2+k_3}[\mathrm{Q}][\mathrm{E_{tot}}]}{\frac{(k_{-3}+k_3)(k_{-1}+k_2)}{(k_2+k_3)k_1} + [\mathrm{Q}]} \approx \frac{\frac{k_2k_3}{k_2+k_3}[\mathrm{Q}][\mathrm{E_{tot}}]}{\frac{k_{-3}+k_3}{k_2+K_3}K + [\mathrm{Q}]} \tag{1.20}$$

The rate of hydrolysis is,

$$\frac{d[\mathrm{P_i}]}{dt} = k_2[\mathrm{ET^{met}Q}] + k_{-3}[\mathrm{E_{tot}}] = \frac{k_{-3}k_3(k_{-1} + k_2) + k_2k_3k_1[\mathrm{Q}]}{(k_{-3} + k_3)(k_{-1} + k_2) + (k_2 + k_3)k_1[\mathrm{Q}]}[\mathrm{E_{tot}}] \tag{1.21}$$

which simplifies to:

$$\frac{d[\mathrm{P_i}]}{dt} = \frac{\frac{k_{-3}k_3}{(k_2+k_3)}K + \frac{k_2k_3}{(k_2+k_3)}[\mathrm{Q}]}{\frac{(k_{-3}+k_3)}{(k_2+k_3)}K + [\mathrm{Q}]}[\mathrm{E_{tot}}] \tag{1.22}$$

When the ATPase rate is rate-limiting: k_2, $k_{-3} \ll$ other rates

$$\frac{d[\mathrm{met}]}{dt} = \frac{k_2[\mathrm{Q}][\mathrm{E_{tot}}]}{K + [\mathrm{Q}]} \tag{1.23}$$

$$\frac{d[\mathrm{P_i}]}{dt} = \frac{k_{-3}K + k_2[\mathrm{Q}]}{K + [\mathrm{Q}]}[\mathrm{E_{tot}}] \tag{1.24}$$

1.5 Introduction to MST and SPR

Here we discuss two commonly used instruments, SPR and MST to study the kinetics and thermodynamics of the different conformations of MetNI during the transport cycle.

Surface Plasmon Resonance (SPR)

From protein biochemistry to environmental safety, molecular binding processes underpin some of the richest avenues of research in a wide array of fields. Although there are a number of other techniques used to study these processes (e.g., ITC and ELISA), surface plasmon resonance (SPR) is an increasingly popular method picked to determine rates and affinities of various interactions between binding molecules, protein-protein and protein-small-molecule in our studies. The application of SPR results in a highly-sensitive technique used for real-time, binding-event monitoring. SPR is valued for its minimal sample consumption, label-free detection ability, higher quality kinetics (i.e., association and dissociation constants, in addition to equilibrium), and faster experiments.

Surface plasmon resonance is a physical, optical phenomenon that can be utilized to observe and record refractive index changes. In the Biacore SPR instrument, analysis of these differences in refractive indexes over time allows for binding, kinetics, affinity, specificity, and concentration studies in a single device. This utility, combined with high sensitivity and high reliability relative to other comparable techniques, made SPR ideal for our studies.

In order to better understand how the SPR technique works, we must first discuss a few concepts. Key to SPR are the free conduction electrons in metals. In interactions between the metal and a driving electric field, these electrons have out-of-phase oscillations with respect to the electric field, which at optical frequencies, give most metals a couple of notable properties. First is a negative dielectric constant, which results in the physical property of having very high reflectivity. Second, and most importantly, there can be charge density oscillations, both volume and surface, in the free electron gas of the metal. Some of these charge density oscillations can be

caused by light.

As we know, light is an electromagnetic wave that has both electric and magnetic fields. These fields oscillate perpendicularly to one another and generally run normal to the direction of motion. When visible light is directed at a conductive metal, the electric field of the light causes free conduction electrons at the surface of the metal to begin vibrating. However, under certain conditions discussed below, a longitudinal wave of electrons can become excited by the light wave, which results in its own electromagnetic wave. This electron density wave, and associated electric and magnetic fields, is called a "surface plasmon" and is confined to the interface between two media with differing refractive indexes. It may be easier to think of a surface plasmon as light "bound" to the surface of a conductive metal and propagating along the surface while presenting as an electromagnetic field.

One particular property of surface plasmons is important to our discussion of SPR: it has a shorter wavelength when compared to light of the same frequency. Since energy is proportional to momentum, we can also say that photons have less momentum than surface plasmons of the same frequency. Therefore, in order to convert a photon into a surface plasmon, additional momentum must be provided according to the conservation of energy and momentum. This conversion of photons into surface plasmons occurs inside the Biacore SPR instrument using the Kretschmann configuration.

The Kretschmann configuration takes a thin metal film (e.g. gold) and places it between two dielectric materials with differing refractive indexes. In the Biacore instrument, a prism is used as the higher refractive index material, while an experiment-specific solution serves as the lower refractive index medium. Plane-polarized light is shone through the prism during SPR. When light travels from a higher refractive index material to one of lower refractive index, a phenomenon known as total internal reflection (TIR) can occur.

When light is directed from the denser (i.e. higher refractive index) material at angles of incidence less than the so-called "critical angle", both refraction into the less dense (i.e. lower refractive index) material and reflection into the denser material occur. As the incidence angle increases, the angle of refraction increases non-linearly at a faster rate and the light that is refracted becomes dimmer (i.e. less refraction), while the reflected light becomes brighter (i.e. more reflection). Once the angle of refraction is equal to or greater than 90°, no light refraction is observable, and all the light is reflected back to the denser medium. The incidence

angle that produces an angle of refraction equal to 90° is the critical angle. Any light shone at an incidence angle greater than the critical angle undergoes TIR. To summarize, there are two requirements for TIR: light must originate from the denser medium and approach the less dense medium, and the angle of incidence must be greater than the critical angle.

Under TIR, reflected photons create an electrical field at the interface between the two media. No energy is actually transmitted across the interface, but the electrical field extends beyond the boundary of the denser medium and into the metal film and the less dense medium. The electrical field component that is normal to the interface is called an evanescent wave. Evanescent waves have amplitude that decrease exponentially with distance from the interface and generally fully decay over one light wavelength. These evanescent waves are critically important to SPR as they serve as the source of excitation for surface plasmons.

The excitation of surface plasmons is also called surface plasmon resonance. In order for SPR to occur, the momentum of the surface plasmons must match the momentum of incident light, also called momentum resonance. Under the right conditions for wavelength, angle of illumination, and refractive index of the media, photons are absorbed and become surface plasmons, which is observable as a "shadow" in the reflected light. This serves as the major mechanism by which the SPR technique functions.

In the Biacore instrument, plane-polarized light is focused into a wedge-shaped beam. This beam is aimed at the "TIR interface", which consists of the prism (i.e. the high refractive index medium) and the sensor chip; the sensor chip contains the gold film and multiple microfluidic channels. The low refractive index medium is the surface coating of the sensor chip and the injected sample solution. The angle of "minimum reflectance intensity", which is the illumination angle that exhibits SPR at the TIR interface, is recorded as a baseline. As various interactions occur on the surface of the sensor chip, solute concentration changes. These changes affect the refractive index of the "low refractive index" medium, which in turn affects the penetration ability of the evanescent waves produced by TIR. A change in the evanescent waves necessitates a change in the angle of incidence of the light in order to exhibit SPR. This difference in angle of incidence is measured as the response signal. Useful depth of detection is about 300 nm. This limits the instrument to only detect close intermolecular interactions.

In summary, SPR can occur when plane-polarized light hits an electrically con-

ducting surface, generally a thin, metal film, at the boundary between two media with different refractive indexes. Under TIR, electrons from the outer shell or conduction-band of the metal film absorb photons from the polarized light to form "surface plasmons". Evanescent waves from totally internally reflected photons causes excitation of these surface plasmons, which results in SPR. SPR is observable as a "shadow" in the reflected light. These SPR shadows are used in the Biacore SPR instrument to generate a response signal that is influenced by biomolecular interactions on the sensor chip surface.

Assay Setup

To make an SPR measurement, it requires a molecule to be immobilized on a sensorchip. The counterpart binding partner flows through the microfluidic channel. They are called ligand and analyte, respectively.

First, the molecular weights of the two molecules need to be considered. The relationship between the response signal and the mass of the ligand and analyte is defined in Equation 1.25. The mass ratio of analyte to ligand should be within the same order of magnitude. Also, it is ideal for the analyte to be larger than the ligand to obtain a robust response. Therefore, SPR is not an appropriate technique to analyze binding interactions that involve a small molecule (e.g. ions) and a macromolecule (i.e. protein).

$$\text{Response(RU)} = \frac{\text{immobilization(RU)} \times \text{analyte(MW)}}{\text{ligand(MW)}} \tag{1.25}$$

The method of immobilization can be through covalent binding or ionic interaction. To immobilize the ligand, the molecules can be added to the sensor surface to bind to high affinity pre-attached molecules, for instance, antibodies, Ni-NTA. Alternatively, molecules can be concentrated to the surface using buffer with a pH lower than the isoelectric point of the protein to form covalent bonds between the protein and the carboxymethylated dextran on the chip.

A sensorgram records the binding interaction over time. A sensorgram consists of three parts, association, equilibrium, and dissociation. The binding curves can be fitted according to a model that describes the reaction measured. Methods of data fitting and evaluation of the fit are discussed in Section 3.4 and 3.5.

Microscale Thermophoresis (MST)

Thermophoresis is an intrinsic property of a molecule where a directed movement occurs in a temperature gradient, dependent on the size, charge, and hydration shell of the molecule. These factors are encapsulated in the Soret Factor, S_T (Duhr and Braun, 2006b; Duhr and Braun, 2006a)). The change in hydration shell can be a result of changes in their primary, secondary, tertiary, and quaternary structures. This behavior of molecules is a deviation from the random distribution of molecules by Brownian motion in equilibrium at a constant temperature.

The directed movement is different when a molecule is bound to another molecule. Therefore, the phenomenon can be used to measure inter-molecular interactions. It is suitable for macro-molecules binding because binding of these large molecules usually causes a change in one or all three of the factors mentioned above. The upper mass limit for macromolecules can be as large as a bacterium. It can also be used to measure an interaction between a macromolecule and a small molecule (e.g. ions and amino acids) because even though the binding of a small molecule might not induce a measurable change in size, it can, however, induce changes in charge and the hydration shell.

The tracking of the directed movement is done by fluorescent labeling of one of the two binding partners. At the start of the measurement, the fluorescently labeled molecules are evenly distributed among the non-labeled molecules at equilibrium. Therefore, this is a steady state measurement. Before a higher temperature is introduced, the binding event has already occurred. Then a small spot within this solution is heated; there is a hot spot within the cooler solution. Simultaneous to heating up a spot, the amount of fluorescence gain (if molecules move towards the hot spot) or lost (if the molecules move away from the spot) on the spot is recorded. The direction that the molecules move is an intrinsic property of that molecule.

The relationship between the change of concentration of the fluorescently labeled molecules in a temperature gradient and the Soret factor is expressed as:

$$\frac{c_{hot}}{c_{cold}} = exp(-S_T \Delta T) \tag{1.26}$$

The MicroScale Thermophoresis Instruments (MST) are manufactured by Nano Temper Inc, a German company. They offer a variety of MST instruments to accommodate inter-molecular interactions that have different binding affinities. The instrument used for the experiments in this thesis is called NT.115. One of the most prominent features of this instrument is the sample solution that is loaded to

a capillary with a width of 10 mm. The length of the capillary does not matter because the cross section of the capillary is heated. Therefore, the volume of the heated spot can be calculated as 10 mm multiplied by the cross section area of the infrared laser, which is small. Therefore, MST consumes a small amount of sample. Each measurement is as long as a fluorescence scan; it takes about 40 seconds of measurement time per titration point.

There are caveats to using MST. MST is an equilibrium measurement that detects a wide range of affinities. It is quick to perform, and thus can be a good starter instrument. However, the readout of MST depends on the Soret factor change from being a lone molecule to be bound to another molecule. The change in Soret factor depends on the size, charge, or hydration shell change upon binding. A binding event can occur but not induce a measurable change in any of the above-mentioned factors, which results in directed movement that is too small to be detected by the fluorescence scanner. Therefore, a limitation of MST is that if such change is too small to create a thermophoresis profile change detectable by the specified fluorescence detector, false negatives can result.

Assay Setup

An MST measurement requires labeling of one of the two partners for the binding interaction. There are two types of commonly used protein labeling strategies: primary amines and maleimide chemistry. Since lysine is abundant in proteins, labeling is often non-specific. It has been shown that non-specific label serves well to record fluorescence change of the heated spot over time. On the other hand, with proteins containing a single or no cysteine, specific labeling can be achieved in some cases.

Data is plotted on a semi-log scale with the y-axis as the binding signal and the x-axis as the concentration of the titrant. The binding curve is either fitted using the K_d equation (Equation 1.27) or the Hill equation (Equation 1.28) to output a dissociation constant and a hill coefficient if applicable.

Fit function for K_d from the law of mass action:

$$A + T \leftrightarrow AT \tag{1.27}$$

$[A_0]$: The concentration of the fluorescently labeled molecules

$[T_0]$: The concentration of the titrated molecule T

[AT]: The concentration of the complex formed by A and T

$$FractionBound = \frac{1}{2[A_0]}([T_0] + [A_0] + K_d - \sqrt{([T_0] + [A_0] + K_d)^2 - 4[T_0][A_0]} \tag{1.28}$$

Fit using the Hill equation.

$$A + nT \leftrightarrow AT_n \tag{1.29}$$

EC_{50} is the concentration of molecule T when half of A is bound to T.

n: Hill coefficient

$$FractionBound = \frac{1}{1 + (\frac{EC_{50}}{[T_0]})^n} \tag{1.30}$$

Chapter 2

TRANSPORT MECHANISMS FOR ABC IMPORTERS

2.1 Introduction

Previous studies of ABC transporters have been heavily focused on the structural determination of the different intermediates of the transport cycle. In this chapter, we place an emphasis on how the conformational changes, from one intermediate to another, drive the transport process and complete the transport reaction. We also analyze how the conformational changes enable the coupling of ATP hydrolysis and substrate translocation.

Prior to discussing the conformational changes of ABC importers, it is important to note that there are two types of importers: Type I and Type II. The subject of my study, MetNI, along with the other well characterized importers $MalFGK_2$, ModBC, and histidine are all Type I transporters. The two most prominent Type II importers are BtuCD and MolBC. These two types were previously classified based on topology and architecture (Goetz, Perozo, and Locher, 2009; Joseph et al., 2011). However, more recently, the field has transitioned to including transport mechanism as a criterion during classification (Locher, 2016). This shift in criterion priority is underpinned by multiple findings. First, transport mechanisms can be identified by the number and type of folds of the transmembrane helices (Vigonsky, Ovcharenko, and Lewinson, 2013). Second, and most importantly, it has been unequivocally demonstrated that Type II importers have distinct conformations, relative to Type I importers, during transport (Lewinson et al., 2010; Locher, 2016). Therefore, since the transport mechanism serves such a vital role in ABC-importer classification, our interest is to elucidate the MetNI Type I transport-cycle.

In this chapter, we develop a framework for the mechanistic analysis of ABC transporters. First, we collate previously reported structural information on the conformational states of ABC importers and associated binding proteins. Then, we summarize the available kinetic and thermodynamic characterization of the transport intermediates. From these considerations, we propose the following mechanism that describes the transport cycle for ABC Type I importers.

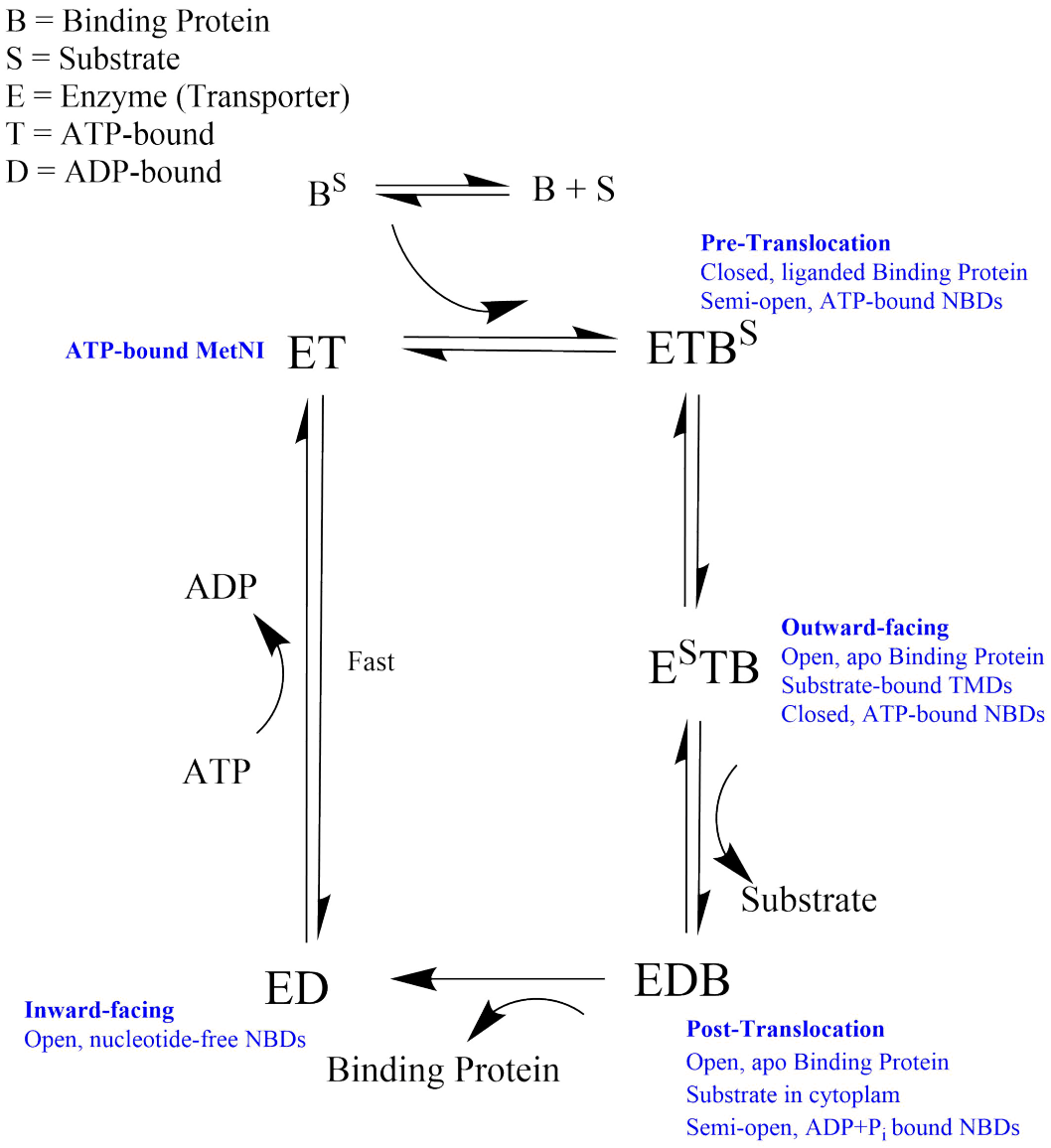

Figure 2.1: **A general transport mechanism proposed for Type I ABC importers**. There are five major enzyme-states during substrate transport, with three states being complexes with a binding protein. The model assumes that the transporter binds to ATP readily to form 'ET'. Transport is initiated when a liganded binding-protein comes in contact with 'ET' to form a protein complex, 'ETB^S', which is the pre-translocation conformation. The Substrate moves from 'B' (binding protein) towards 'E' (Enzyme, transporter) to form 'ET^SB', which is the outward-facing conformation. After the substrate is translocated to the cytoplasm, ATP is hydrolyzed yielding the post-translocation state, which is bound with ADP and Pi. ATP replaces ADP in the transporter and a new transport cycle can start.

2.2 Binding Protein Conformations

Substrate translocation by ABC importers is dependent on periplasmic binding proteins that have a high affinity for substrate. The binding protein binds to substrate

that enters into the periplasmic space and carries it to the membrane to interact with the appropriate transporter. Here, we discuss four important points related to binding proteins relevant to understanding the ABC import mechanism: 1) the reasons why they are essential for transport; 2) their structural architecture; 3) X-ray structures of the binding proteins for the most well-characterized Type I and Type II ABC transporters; and 4) binding proteins can form a complex with the transporter in two different conformations.

Prokaryotic ABC importers are dependent on binding proteins; we discuss the reasons why they are essential. First, when the concentration of nutrients and ions that enter into the periplasm is low, a high-affinity binding protein sequesters the substrate for transport. Biochemical studies show that the affinity of the binding protein substrate site is high, in the pM - nM range. Binding proteins are also important due to their ability to stimulate ATPase activity of the transporter, as shown originally in histidine permease studies (C. E. Liu et al., 1999). Therefore, periplasmic binding proteins are essential for substrate translocation not only because of their affinity to sequester substrate for transport but also their ability to stimulate ATPase activity.

Structurally, the binding proteins of ABC transporters consist of two domains (or lobes), the N- and C-domains (Berntsson et al., 2010). There is a cleft formed by a flexible hinge that connects the two domains (Spurlino, G. Y. Lu, and Quiocho, 1991). The opening and closing of these two lobes create two major conformations (Sharff et al., 1992; Quiocho, 1990). The conformational change from the open to the closed state is facilitated by the binding of the substrate to the binding protein. Once substrate binds to the open state of a binding protein, the two domains of the binding protein come in close contact with each other to form a substrate binding site that occludes the substrate. The binding protein can form a complex with the transporter in both its open or closed state.

There are structures of many binding proteins available. Here we describe the binding protein of the most well-characterized ABC importers (Table 2.1) (Hollenstein, Frei, and Locher, 2007; Nguyen et al., 2015; Higgins and Ames, 1981; Oldham, S. Chen, and J. Chen, 2013; Kim et al., 2013; Gouridis et al., 2015). For example, the structural determination of the methionine binding protein MetQ occurred with L-methionine bound (Nguyen et al., 2015). The maltose binding protein MalE has been structurally determined in complex with the maltose transporter both in apo- (Oldham, Khare, et al., 2007; Oldham and J. Chen, 2011b) and bound-state (Oldham and J. Chen, 2011a). As discussed later, though the Type II importers operate using

a fundamentally different mechanism, the structures and functions of the binding proteins are comparable. For example, the structure of an open BtuF was found to be in a complex with a post-T transporter (Hvorup et al., 2007; Korkhov, Mireku, and Locher, 2012).

2.3 The Conformational States of ABC Importers

Type I ABC Importers

For our discussion, we begin by defining four conformational-states based on crystallographic analysis: the pre-translocation (pre-T), outward-facing (outward), post-translocation (post-T), and inward-facing (inward) conformation. Three of these conformations—pre-T, outward, and post-T—are transporter-complexes that have formed a complex with the binding protein. The pre-T conformation is bound to a liganded binding protein, while the outward and post-T conformation are bound to an apo binding protein. The pre-T and outward conformation are ATP-bound, while the post-T conformation is ADP- and Pi-bound. The inward state is nucleotide-free.

The study of ABC transporters has been guided by the alternating access model, which stipulates that to translocate substrate, the transporter opens towards one side of the membrane to load the substrate, then switches the opening to the other side of the membrane to unload. Specifically, the opening of the transporter is done through the opening of the TMDs towards either side of the membrane. Therefore, it is crucial to define the conformations of the TMDs. The substrate binding site formed by the TMDs is called the translocation pathway substrate binding site ('translocation pathway site'). The alternating access model stipulates that there are two major conformations of the cavity formed by these two TMDs and the orientation of the opening in relation to the membrane (Jardetzky, 1966). The outward-facing orientation of the TMDs forms a cavity which opens to the periplasm, while inward-facing TMDs have the cavity open toward the cytoplasm.

The translocation pathway site has been observed in the maltose system (Oldham, Khare, et al., 2007; Oldham and J. Chen, 2011b; Oldham and J. Chen, 2011a; Oldham, S. Chen, and J. Chen, 2013) and an amino acid ABC importer Art$(QN)_2$ (Yu et al., 2015). The maltose translocation sites were characterized to have a K_d of 2 mM from a MBP-independent MalFGK$_2$ mutant study where this mutant has its specificity for maltose unchanged (Cui, Qasim, and Davidson, 2010). This observation showed that this site has a low affinity compared to the binding protein substrate site. The low affinity of this site again emphasizes the importance of a

high-affinity periplasmic binding protein to assist transport.

Type I	**Pre-T**			**Outward-facing**			**Post-T**			**Inward-facing**		
Parameters	k_1	k_{-1}	K_d	k_1	k_{-1}	K_d	k_1	k_{-1}	K_d	k_1	k_{-1}	K_d
Unit	$M^{-1}\,s^{-1}$	s^{-1}	M	$M^{-1}\,s^{-1}$	s^{-1}	M	$M^{-1}\,s^{-1}$	s^{-1}	M	$M^{-1}\,s^{-1}$	s^{-1}	M
Binding Protein	closed			open			open			not in complex		
TMDs	inward			outward; substrate-bound			inward			inward		
NBDs	ATP; Semi-open			ATP; closed			ADP-Pi; Semi-open			nucleotide-free; open		
MetNI	2×10^4	0.03	6×10^{-7}	1×10^3	1×10^{-5}	1×10^{-8}	NR			No Asso(ADP, Se-met)		
$MalFGK_2$	NR	NR	NR	NR	NR	2×10^{-6}	ADP-Vi			No Association		
Histidine	NR	NR	NR	NR	NR	1×10^{-8}	NR			No Association		
AfModBC	5×10^4	0.2	4×10^{-6}	2×10^3	$3\times10^{-3}4$	1×10^{-6}	1×10^3	5×10^{-4}	5×10^{-7}	No Association		
Type II	**Outward**			**Inward**			**Post-T**			**Resting**		
Binding protein	Absence			apo			apo			apo		
TMDs	outward			inward			inward			inward		
NBDs	ATP, closed			ATP, closed			$ADP+P_i$, semi-open			open		
hiMolBC	No Association			NP			3×10^5	9×10^{-4}	3×10^{-9}	3×10^4	9×10^{-4}	2×10^{-8}
BtuCD	No Association			9.5×10^3	2.0×10^{-6}	1.07×10^{-11}	5.5×10^4	2.0×10^{-6}	1.7×10^{-11}	4.5×10^4	1.1×10^{-8}	1.1×10^{-13}

Table 2.1: **A summary of the characterization of different conformations for ABC importers.** For Type I importers, the major conformations include the Pre-T, outward, Post-T, and inward conformation. For Type II importers, the major conformations include outward, inward, post-T, and resting state. Some of these conformations have been characterized biophysically and others structurally by x-ray crystallography. Some kinetic measurements were reported. k_1 and k_{-1} is the rate constant for complex association and dissociation, respectively. K_d is the dissociation constant. 'NR' means not reported. The histidine transporter is not discussed elsewhere; its reference is (P. Q. Liu, C. E. Liu, and Ames, 1999; P. Q. Liu and Ames, 1998). All measurements for the other transporter are reference in the text. HiMolBC: (Vigonsky, Ovcharenko, and Lewinson, 2013) AfModBC: (Vigonsky, Ovcharenko, and Lewinson, 2013) AfModBC: (Tomatsu et al., 2007)

The Pre-translocation Conformation

The key features of the pre-T state are (as seen in Table 2.1): a closed, liganded binding protein that is bound to the transporter; the TMDs of the transporter are inward-facing; and the NBDs are semi-open (Oldham and J. Chen, 2011a; Hollenstein, Frei, and Locher, 2007). Even though the pre-T state has been observed to be nucleotide-free in crystal structures, SPR studies of the MetNI shows that the binding protein does not form a complex with the transporter in the absence of ATP, therefore, without ATP bound to the NBDs, the pre-T conformation cannot be established. We hypothesized that the pre-T state either has one or both ATP bound to the NBDs. We will describe evidence for these features and their mechanistic importance.

A closed, liganded binding protein bound to the transporter is supported by pre-T crystal structures of the maltose transporter (Oldham and J. Chen, 2011a) and $ModB_2C_2$ transporter (Hollenstein, Frei, and Locher, 2007). The binding protein hands over the substrate to the transporter, which initiates a series of events that facilitate transport and hydrolysis. These features of the binding protein have two putative importance to the transport mechanism. First, the binding protein is predicted to stimulate ATP hydrolysis. Second, the bound substrate is predicted to stimulate the release of P_i (Bao, Dalal, et al., 2015). Therefore, the pre-T conformation has set the stage for ATP hydrolysis.

Studies show that the TMDs are inward-facing (Oldham and J. Chen, 2011a). It is hypothesized that the liganded substrate triggers the conformational change of the TMDs from inward to outward-facing—a key feature of the outward state, which follows the pre-T state. Therefore, the interaction of the liganded binding protein with the inward-facing TMD is an important step in promoting the continuation of the transport cycle.

The semi-open NBDs signal that this state is not yet poised for hydrolysis to occur. In the $ModB_2C_2$ system, the structure of an intermediate state showed semi-open NBDs (Hollenstein, Frei, and Locher, 2007). The closing of the NBDs will promote the transporter to proceed to the outward state. Though there is controversy over what molecular events precipitate the closing of the NBDs (Orelle, Ayvaz, et al., 2008; Bao and Duong, 2013), generally, we believe that binding of both ATP to the NBDs is the trigger. It is hypothesized that the closure of NBDs is concomitant to the change of inward-facing TMDs to outward-facing.

Some observations complicate the features of the pre-T state. For instance, the translocation pathway site is supposed to be vacant in the pre-T state because the substrate is still bound to the binding protein. However, the pre-translocation conformation of $MalFGK_2$ has a second maltose molecule in the translocation pathway site (Oldham and J. Chen, 2011a). Even though this maltose is not likely to be present in this conformation—presumably, an artifact of the high concentration of maltose used during crystal preparation—this structure does show the presence and the location of a TMD substrate binding site.

The Outward-facing Conformation

The key features of the outward conformation are: an open, unliganded binding protein is bound to the transporter; the two TMDs are outward-facing and the substrate is occluded in the cavity formed by the TMDs; the two NBDs are closed and ATP-bound. Below we discuss the evidence and mechanistic importance of these features.

An open, unliganded binding protein bound to the transporter is supported by studies where MalE is in the open conformation during the catalytic transition state for ATP hydrolysis via EPR (Austermuhle et al., 2004; J. Chen et al., 2001). When the transporter is bound to an open binding protein (Oldham, Khare, et al., 2007; Khare et al., 2009; Oldham and J. Chen, 2011b), it indicates that the substrate has already dissociated from the binding protein and is bound to the translocation pathway site of the transporter complex. The observation that the liganded binding protein in the pre-T state possibly indicates that when a liganded binding protein binds, the bound substrate interacts with the transporter and triggers a conformational change to close the semi-open NBDs.

This unliganded binding protein is shown to form a complex with ATP-bound MetNI with high affinity. For example, $MalFGK_2$ forms a complex with the closed MalE with an affinity of greater than 45 μM, while it is 60 nM with the open unliganded MalE (Table. 2.2) (Bao and Duong, 2012; Bao and Duong, 2013). This observation is also true for the MetNI system (in Chapter 3). The different affinities imply that the outward state has a higher affinity than the pre-T state, if both states can be experimentally trapped. The hypothesized molecular significance of the outward state having a higher affinity is the creation of a stable condition/platform for substrate translocation and ATP hydrolysis to occur and to favor transfer of ligand from the binding protein to the transporter.

The TMDs are outward-facing, and the substrate is occluded in the cavity (Oldham, Khare, et al., 2007). It is believed that the closure of the NBDs is concomitant with the substrate dissociating from the binding protein and binds to the translocation pathway site in the transporter (Oldham, Khare, et al., 2007). Therefore, the three molecular events—the closure of NBDs, the conformational change of TMDs from outward to inward-facing, and the substrate binding to the translocation pathway site—are essential for proceeding to the post-T state to achieve substrate translocation.

A prominent feature of this state is that the transporter has closed, ATP-bound NBDs that are ready for hydrolysis. The closing of the NBDs necessitates the conformational change from the pre-T to the outward state. However, there is no consensus on the conditions for closure. Davidson et al determined that both MalE and ATP binding are required for NBD closure using EPR (Orelle, Ayvaz, et al., 2008). Conflictingly, Bao and Duong showed that ATP alone triggers the outward state of the maltose ABC transporter and that the binding of MalE is not required (Bao and Duong, 2013). Nonetheless, it is agreed that when the two NBDs have moved closer to each other, the transporter is in its outward state.

	Open-state	Closed-state
$MalFGK_2E$	60 nM	> 45 μM
MetNIQ	25 nM	1100 nM

Table 2.2: Both MetNI and $MalFGK_2$ forms a complex with a higher affinity with their respective binding protein in an open, unliganded state than the closed-state (Bao and Duong, 2013).

The Post-translocation Conformation

The key features of the post-T state are as follows: an open, unliganded binding protein is bound to the transporter; the two TMDs of the transporter are inward-facing; the two NBDs are semi-open and ADP and P_i-bound.

It was shown via EPR studies that when the complex is stabilized, using non-hydrolyzable MgATP analogs or ATP in the absence of Mg, the binding protein is in the open state and bound to the transporter (Austermuhle et al., 2004). The importance of this feature is supported by the results of the Duong group, which suggest that the bound binding protein stimulates ATP hydrolysis (Bao, Dalal, et al.,

2015). Hydrolysis will provide energy for conformational change and substrate translocation.

The inward-facing orientation of the TMDs is supported by X-ray crystallography structures of the post-T state of the maltose transporter (Oldham and J. Chen, 2011b). This state was stabilized by ADP in conjunction with phosphate analogs. The two halves of the now inward-facing TMDs were shown to form a substrate binding site that occludes a maltose molecule.

To stabilize the post-T complex, the products of hydrolysis (i.e. ADP and P_i) must be trapped within the NBDs. Therefore, the nucleotide state of the post-T conformation requires both ADP and P_i. ADP alone is not enough to stabilize a transporter complex (Orelle, Ayvaz, et al., 2008; Karpowich et al., 2001; G. Lu et al., 2005). The release of P_i triggers the opening of the NBDs; we saw in the inward-facing conformation of MetNI, that the NBDs are ADP-bound (with P_i has been released) and open (Kadaba et al., 2008).

In conclusion, after the important molecular event of substrate translocation, the separation of the NBDs helps to reset the transporter for a new cycle. It is predicted that the release of ADP and P_i destabilizes the closed NBDs. As soon as ADP and P_i are released, the NBDs further widens to allow ATP to reload the transporter.

The Inward-facing Conformation

The inward state is distinct from the pre-T, outward, and post-T states in that the binding protein has dissociated. The two TMDs are inward-facing while the NBDs are open, in either nucleotide-free or ADP-bound form.

Three structures (2ONK, 3D31, 3DHW) of the inward-facing conformation have nucleotide-free NBDs (Johnson et al., 2012; Kadaba et al., 2008; Pinkett et al., 2007; Khare et al., 2009). However, one of the structures for the inward-facing conformation of MetNI shows that ADP is bound (Johnson et al., 2012). This could be because the inward state can be stabilized in a range of NBD separations, as well as nucleotide states (Kadaba et al., 2008). Importantly, the observation of the bound ADP to the MetNI inward-state suggests that the dissociation of P_i triggers separation of the NBDs and shift the transporter to the inward facing conformation.

EPR studies also show that the NBD interface is open when no nucleotide is bound (Orelle, Ayvaz, et al., 2008). After the release of ADP and P_i, the NBDs become open and free to bind ATP to start a new cycle.

Type II ABC Importers

During the substrate translocation cycle, the conformations for Type II are distinctly different from Type I. The cycle starts with the outward state, proceeds to the inward state, to the post-translocation state to resting state.

The outward-facing conformation

The outward-facing state has closed ATP-bound NBDs. The periplasmic gate of the TMDs (i.e. the peri-gate (Locher, 2016)) are open, hence, this state is called "outward-facing". Since the outward state is not bound to a binding protein, it is not ready for substrate translocation. However, the closed-, ATP-bound NBDs are poised for ATP hydrolysis; this explains why Type II importers have high basal rates of hydrolysis (Borths et al., 2005).

It is predicted that the transporter is ATP-bound (Locher, 2016) even though there are structures of outward-facing conformation with nucleotide-free NBDs for the BtuCD (Locher, Lee, and Rees, 2002).

The Inward-facing conformation

The binding of a liganded binding protein to the outward state of the transporter triggers a conformational change to the inward state in order to facilitate substrate translocation. Consequently, the peri-gate is closed. In this state, the transporter has closed, ATP-bound (ATP analog, AMP-PNP) NBDs; the TMDs have rearranged, and space is made available to occlude a substrate (Korkhov, Mireku, and Locher, 2012). The transporter is now in complex with an apo binding protein as the substrate has translocated to the TMDs (R. J. P. Dawson and Locher, 2006).

The post-Translocation Conformation

Upon ATP hydrolysis, the transporter adopts the post-translocation state. This state has semi-open, ADP- and Pi-bound NBDs in association with an open, apo binding protein. It is predicted that at this state, the substrate is still bound in the translocation pathway site. This conformation corresponds to the complex at 1.76×10^{-11} M measured by SPR (Lewinson et al., 2010) with ATP, Mg^{2+}, and vanadate.

Subsequently, the dissociation of the open, apo binding protein promotes the transporter to return to the outward conformation, which is ready to load ATP molecules

for a new cycle.

The resting Conformation

The transporter can also adopt the resting state, where it is bound to an open, unliganded binding protein (Locher, Lee, and Rees, 2002). It is substrate-free and nucleotide-free.

This conformation corresponds to the complex with the highest affinity at 1.16×10^{-13} M measured by SPR (Lewinson et al., 2010). Only one condition, (ADP + Mg^{+2} gives the same level of magnitude as BtuCD-F alone (Rees, Johnson, and Lewinson, 2009). Since ADP alone does not stay stably within the NBDs without Pi, what is most likely being measured here is BtuCD forming a complex with BtuF in the absence of all additives. A new transport cycle starts when the dissociation of the open, apo binding protein promotes the transporter return to the outward-facing conformation.

2.4 The Advantages of a Binding Protein

In general, transport does not require a binding protein. ABC exporters and binding protein independent variants of mature ABC transporters do not have binding proteins (Treptow and Shuman, 1985). Neither do secondary active transporters that move solutes toward a higher concentration via symport or antiport of another solute, which moves down the concentration gradient. For instance, LacY, which is a symport of a galactoside and H^+ does not have a binding protein. What do ABC exporters and secondary active transporters have in common that compensates for the lack of a binding protein?

We propose that a possible role of a binding protein is to sequester substrate in order to increase the local concentration of the substrate to make it favorable for transport (Piperno and Oxender, 1968). Sequestering substrate is especially necessary when substrate concentration is low. This is similar to hemoglobin binding to oxygen, when binding of O_2 to a carrier protein increases the total concentration beyond that of the solubility limit of O_2 in water. We propose that ABC importers rely on binding proteins to increase the local substrate concentration for transport.

We propose a secondary explanation that an importer can be promiscuous when it comes to its association to binding proteins; importers can be paired with multiple binding proteins, each of which binds to a range of substrates for transport. This pairing system enables an importer to translocate a variety of substrates so that

cells can be energetically conservative in integral membrane motors synthesis and instead rely on multiple smaller size soluble binding proteins. For instance, Gould and Shilton used mutant sMBP that bind to either maltose and sucrose to demonstrate the ability of sMBP to stimulate ATP hydrolysis as being essentially the same as wild-type MBP, suggesting that the substrate possibly not interact extensively with the transporter during the cycle. It is between the transporter and the binding protein that determines the transport. As such, it is possible that the transporter would interact with a binding protein with little to no regard for what the substrate is (Gould and Shilton, 2010).

As to why ABC exporters do not have a binding protein, exporters move solutes from inside the cell to the outside. The volume of a cell is a small definite space. Therefore, the exporters have an intrinsic mechanism to increase local substrate concentration. Importers, however, transport solutes from outside the cell through the the periplasm to the cytoplasm. Since the outer membrane is semi-permeable, the space where the substrate is for importers is infinite.

Chapter 3

THERMODYNAMIC ANALYSIS OF METNI INTERMEDIATE STATES

3.1 Introduction

ATP-binding cassette (ABC) transporters comprise one of the largest, ubiquitous superfamilies of integral membrane proteins (Linton and Higgins, 1998; Ames et al., 1992). These integral membrane proteins derive energy from ATP binding and hydrolysis to drive the active transport of a variety of substrates across the membrane.

Though the proper function of ABC transporters is important to many biochemical processes, the mechanism of transport has been elusive. An extensive body of qualitative experimental data supports a "two-state, alternating access" model that depicts two major conformations. Each conformation has a substrate binding site—formed by a specific arrangement of the two TMDs—which opens towards one side of the membrane or the other (Jardetzky, 1966). The translocation of substrate across the membrane is achieved through conformational changes coupled to nucleotide state.

Structural studies have informed us about four specific arrangements of the transporter during the transport cycle (J. Chen et al., 2001; Oldham, Khare, et al., 2007; Khare et al., 2009; Orelle, Alvarez, et al., 2010; Oldham and J. Chen, 2011b; Oldham and J. Chen, 2011a; Jin et al., 2012; Locher, Lee, and Rees, 2002; Korkhov, Mireku, and Locher, 2012). First, the pre-translocation (pre-T) conformation was determined to have semi-open NBDs that associate with a closed binding protein. Second, the outward-facing (outward) conformation of the transporter has closed, ATP-bound NBDs that associate with an open binding-protein. Third, a post-translocation (post-T) conformation was determined to have ADP+Pi-bound NBDs that associate with an open binding-protein. Lastly, the inward-facing (inward) conformation has open, nucleotide-free NBDs and is not associated with a binding protein. Considering the structural conservation of the NBDs in these intermediates, NBDs must play a vital role during the transport cycle.

With this background in mind, we begin our discussion of MetNI, an ABC transporter. The import mechanism developed for MetNI has benefited from the knowl-

edge of other systems, like the maltose and vitamin B_{12} ABC transporters. Here, we study MetNI in detail, aiming to elucidate its mechanism. Because of the homology, we hope the MetNI mechanism has predictive power towards other ABC importers.

MetNI is present in *E. coli*, a gram-negative bacteria (Kadner and Watson, 1974), which are distinguished by their double membranes. The double membranes consist of an inner membrane, outer membrane, and the periplasm, the region separating the two membranes. The outer membrane is porous and highly permeable—due to the presence of porins and related molecules—and serves as the entry-point for nutrient-substrates, like amino acids and vitamins. In contrast, the inner membrane forms a permeability barrier that, with the exception of a few small, non-polar molecules, impedes the passage of virtually all molecules into cells.

Nutrient-substrates, like L-methionine, can only gain entry into cells through the action of transporters, like MetNI. These transporters are integral membrane proteins that sit in the inner membrane and move substrates from the periplasm to the cytoplasm. Most substrates transported by ABC importers are in low concentration in the environment, which makes it difficult for transporters to secure nutrients for transport. Predictably, importers have ways to address this shortcoming.

Transporter binding-proteins, like MetQ, can diffuse freely in the periplasm and have a high affinity for nutrient-substrates (Kellermann and Szmelcman, 1974; Ferenci et al., 1986). For example, when a binding protein captures a substrate under physiological conditions, the high affinity means it is favorable for L-methionine to be bound to MetQ—in all the conditions we have tested, other than through the transport process, MetQ releases L-methionine only under refolding conditions. Therefore, binding proteins help serve as a sequestering agent for transporters and gather much-needed nutrient substrates.

MetQ serves two major functions for MetNI. First, MetQ acts to sequester nutrient-substrates when they enter the periplasmic space. Second, it delivers methionine to the MetNI transporter to create a uni-directional mechanism to move substrates from the periplasm into the cytoplasm. The affinity of MetQ for methionine is clearly critical to fulfilling these functions and therefore, we aimed to quantify MetQ's affinity for L-methionine experimentally.

MetQ binding to L-methionine is only the beginning of transport, and we wish to characterize the transport mechanism further. Therefore, we characterized and isolated certain intermediate states of MetNI during the transport cycle and used

this information to propose a kinetic model of ABC transporter function. We used SPR and MST to study the dynamics and energetics of the transport cycle.

Based on this analysis of the interactions of MetQ with MetNI and L-methionine under different conditions, we develop a transport mechanism that is a synthesis of previous experimental observations and present kinetic and thermodynamic characterizations. With this approach, we quantified the nature of the translocation states, measured the affinities for substrate binding sites, and analyzed the nature of the regulatory transinhibition mechanism. Overall, we are interested in exploring: (1) L-methionine binding to MetQ (2) the kinetics and equilibrium constants for the formation of major intermediate conformations of the transporter during substrate translocation, (3) the mechanism for transinhibition, and (4) the advantages of having a binding protein.

We used SPR and MST because both techniques provide quantitative measurements of the relative stabilities of different conformations. SPR, in particular, can measure the rate constants of complex association and dissociation; as well as affinities. MST provides affinity data, not kinetic data; however, an MST setup is different from the SPR microfluidics setup and enables us to measure reactions that are not possible with SPR.

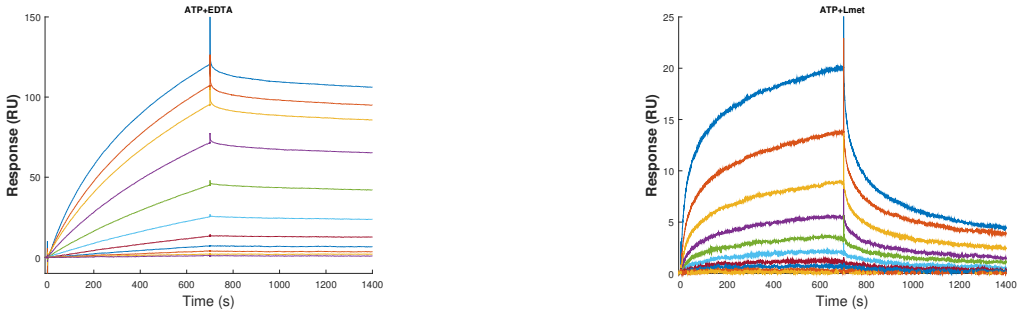

(a) ATP (b) ATP + L-methionine

Figure 3.1: **L-methionine binding MetQ decreases the stability of the MetNI-MetQ complex.** The effect of L-methionine on the MetNI-MetQ system was examined by comparing the kinetics of this complex between ATP- and ATP+L-methionine-containing buffer. By comparison, L-methionine increases the rate constant of dissociation, therefore decreases the complex stability. Panel (a) measurement was done by immobilizing the unfolded-refolded MetQ (an equivalence of 100 R.U. of MetQ) on a Biacore sensor-chip. For the first 700 seconds of the assay, varying concentrations of the construct E166Q MetNI (varying from 1 to 1000 nM) were solubilized in the running buffer (0.025% DDM, 25 mM TAPS pH 8.5, 250 mM NaCl, 1 mM ATP, 1 mM EDTA) and injected to allow interaction with MetQ. The following 700 seconds was a washing step with the aforementioned running buffer. Panel (b) measurement was done with the above SPR setup and the following buffer condition: 0.025% DDM, 25 mM TAPS pH 8.5, 250 mM NaCl, 1 mM ATP, 1 mM EDTA, and 1 mM L-methionine. Each measurement was done in triplicate (see "Experimental Procedure").

3.2 Results

L-methionine binding to MetQ

We wanted to measure the binding affinity of L-methionine to MetQ. However, as discussed below, a method that directly measures this interaction was not available. Therefore, we designed an indirect SPR assay while taking some factors into consideration. First, MetQ and L-methionine are not a good ligand-analyte pair for Biacore kinetic assays—the molecular weight change when methionine binds to MetQ is insufficient to detect by SPR. Second, MetQ binding to L-methionine could not be observed with MST—the change in size, charge, and hydration shell of MetQ upon binding to L-methionine is also insufficient to generate a thermophoresis profile compared to apo-MetQ. Third, the binding affinity of MetQ and L-methionine was too high to study using isothermal titration calorimetry. Therefore, to probe this interaction, we need to look at how L-methionine binding to MetQ affects the MetNI-MetQ system.

It turns out that L-methionine binding to MetQ decreases the stability of the MetNI-MetQ complex. Size exclusion chromatography studies show that the co-purified L-methionine in MetQ decreases the complex's affinity (Nguyen et al., 2015). Our Biacore observations confirmed this notion (Figure. 3.1). In a Biacore assay, MetNI is solubilized in a running buffer containing 1 mM L-methionine. When this L-methionine containing buffer flows over the immobilized apo MetQ, it caused the complex to rapidly dissociate, showing that L-methionine destabilizes the MetNIQ complex. Therefore, we used the MetNIQ complex as a readout for measuring L-methionine binding to MetQ.

L-methionine has three potential binding sites with a complex: MetQ, the MetNI C2 domain, and potentially the MetNI translocation-pathway. Consequently, we used mutations that inhibit the binding of L-methionine to the other two sites to specifically examine binding to MetQ. We used mutation N295A (mutant contributed by P. Nyugen)—located in the C2 domain and prevents L-methionine from binding to C2—to study the interaction between MetQ and L-methionine. There is no mutation available to silence the translocation-pathway binding to L-methionine. However, it is likely that this site has a very low affinity to the substrate, since it has never been observed crystallographically and binding to L-methionine occurs predominantly in the C2 site once the MetQ site is mutated. Therefore, we created conditions that allowed us to inspect the L-methionine site in MetQ.

The second obstacle to measuring MetQ binding L-methionine is that wild-type MetQ co-purifies with L-methionine. This co-purification implies that the MetQ sites are occupied at the start of any experiments, which prevents titrated L-methionine from binding to MetQ. Therefore, we used a high concentration of guanidinium chloride to unfold and then refold MetQ (the unfolded-refolded "Lo" construct of MetQ), which stripped away the bound L-methionine. This process makes the MetQ site available for binding L-methionine.

It is important to establish that the unfolded-refolded MetQ construct has no artifacts that resulted from the unfolding process. We can confirm this by demonstrating that MetQ devoid of L-methionine—via either being washed-away or unfolded-refolded—retains its activity. It has shown that both N229A MetQ and unfolded-refolded MetQ binds to E166Q MetNI with comparable affinities in SPR as well as MST measurements.

In our setup, a constant concentration of transporter flowed above the immobilized MetQ. Based on our observation and upon association of liganded MetQ to MetNI—

in the presence of ATP—the co-purified L-methionine should be transported and washed away in the SPR microfluidic channel. This implies that the majority of MetQ should be in apo form after the first several runs with MetNI.

L-methionine being washed away explains why the wild type MetQ binds to MetNI with the same affinity as the unfolded-refolded MetQ or the N229A MetQ—both constructs are largely devoid of L-methionine (Figure 3.2). The possibility of L-methionine washing away from wild-type MetQ also explains why we observed complexes with the same affinity and kinetic profile whether we started with apo- or liganded-MetQ. The fact that any of the three MetQ constructs always produces a MetNI-MetQ complex with the similar affinities suggests that MetQ is apo because apo MetQ forms a higher affinity complex than liganded MetQ (data shown in MST study below). Therefore, it does not matter whether L-methionine is bound to MetQ at the start of each measurement, as it will dissociate and open up the binding site.

SPR	k_1	k_{-1}	k_2	k_{-2}	K_d
Unit	$M^{-1}\,s^{-1}$	s^{-1}	s^{-1}	s^{-1}	M
N229A MetQ (Red Curves)	2.3×10^3	8.0×10^{-3}	8.6×10^{-3}	1.6×10^{-4}	6.5×10^{-8}
Regular MetQ (Blue Curves)	1.8×10^3	8.8×10^{-3}	9.6×10^{-3}	2.4×10^{-4}	1.2×10^{-7}
Unfolded Refolded MetQ (Green Curves)	2.2×10^3	1.2×10^{-2}	8.8×10^{-3}	2.4×10^{-4}	1.2×10^{-7}

Table 3.1: **Different variants of MetQ behave similarly kinetically.** According to the two-state model, k_1 and k_{-1} are the forward and reverse rate constant for MetNI-MetQ complex formation, respectively. k_2 and k_2 are the forward and reverse rate constant for an isomerization step, respectively. K_d is the dissociation constant for MetNI and MetQ forming MetNI-MetQ according to the Equation 3.2.

We developed the following approach to measure the effect of L-methionine binding to MetQ. We used transporter mutant E166Q MetNI for all of the following assays. MetNI contains a glutamic acid in the Walker B region that takes an active part in facilitating hydrolysis, and the ATPase activity can be significantly inhibited by substitution of this residue by a glutamine (Moody et al., 2002). Mutant E166Q MetNI has been shown to have a 20-fold reduced rate of hydrolysis (work by J. Yang, unpublished). In combination with saturating concentrations of ATP and EDTA, this mutant has been used in other ABC transporters to stabilize the ATP-bound NBDs.

To perform the designed assay, we established a readout by forming a stable complex between the ATP-bound N295A E166Q MetNI and unfolded-refolded MetQ; we

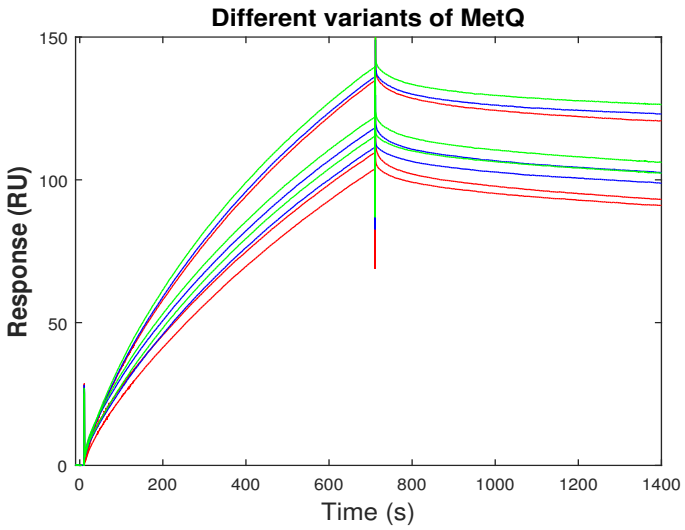

Figure 3.2: **Different variants of MetQ binds to MetNI with the same affinity.** In SPR studies, the affinity of the MetNIQ complex is the same with all three variants of MetQ: (a) Liganded MetQ: wild-type MetQ with co-purifying L-methionine, K_d 1.20×10^{-7} M; (b) Unliganded MetQ: MetQ has been unfolded and then refolded to strip away co-purified L-methionine, K_d 1.27×10^{-7} M; and (c) Unliganded MetQ: N229A MetQ, K_d 0.65×10^{-7} M. In addition to their comparable affinity, the kinetic profiles are also the same. This indicates that all three versions of MetQ, despite having different ligand states when immobilized, end up having the same ligand state in the recorded results. We believe that the L-methionine has been washed away after a few measurements in the SPR microfluidic channel. Experimental setup: on the four channels of the sensor chip, the following were immobilized respectively: the control BtuF, wild-type MetQ, unfolded-refolded MetQ, and N229A MetQ. A constant concentration of E166Q MetNI solubilized in the running buffer (25 mM TAPS, pH 8.5, 250 mM NaCl, 0.025% DDM, 1 mM ATP, and 1 mM EDTA). E166Q MetNI was injected to interact with MetQ in a time- and speed-controlled manner. After each injection, a glycine solution of pH 2 was used to wash off the bound E166Q MetNI. MetQ was tested to be stable under this washing condition. Measurements with each MetQ construct were done in triplicates. This procedure was done for each of the Biacore experiments discussed in the text.

then titrated in L-methionine. First, we immobilized unfolded-refolded MetQ on a Biacore (GE Healthcare) carboxymethylated dextran sensor chip. A covalent bond is formed between the primary amino groups (RNH2) of MetQ via the NHS/EDC activated carboxylate group on the chip. Following immobilization, we titrated L-methionine—along with a constant concentration of E166Q MetNI in each titration injection (solubilized in detergent (0.025% DDM) containing 1 mM ATP and 1 mM EDTA)—onto the flow cells. As a control, we flowed 1000 nM E166Q MetNI over MetQ in the same buffer but without any L-methionine. This obtained a

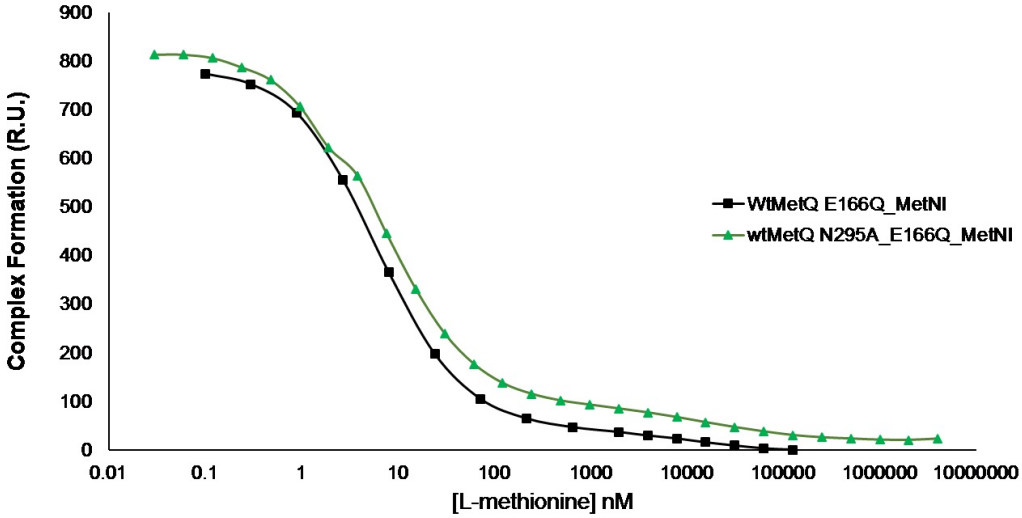

Figure 3.3: **The K_d for L-methionine binding to MetQ is 1×10^{-8} M.** To measure the binding affinity of L-methionine to MetQ, wild-type MetQ was immobilized on a sensor-chip. A binding curve was generated by titrating varying concentrations of L-methionine, with each titrant having the same concentration of E166Q MetNI (1 µM), solubilized in the running buffer (25 mM TAPS, pH 8.5, 250 mM NaCl, 0.025% DDM, 1 mM ATP, and 1 mM EDTA). The black line is generated with the use of the E166Q MetNI; The green line is generated with the double mutant of N295A E166Q MetNI. For both curves, at around 1×10^{-8} M, half of the MetNI-MetQ complex dissociated. There are potentially three binding sites with the E166Q MetNI: MetQ, TMD, and C2. It is predicted that the 1×10^{-8} M is the affinity for MetQ binding L-methionine since the TMD, and C2 sites have much lower affinities.

robust response representing complex formation. Once the injection was terminated at 700 seconds and the washing buffer was started, the complex was stable and did not dissociate. This indicates that a stable MetNI-MetQ was formed with saturating concentrations of ATP and EDTA in the absence of L-methionine. With L-methionine titration, the complex level decreases.

The assay results (Figure. 3.3) showed that MetQ binds L-methionine with high affinity. We did two experiments to confirm the affinity. The first measurement (black curve) is when wild-type MetQ was immobilized with E166Q MetNI (solubilized in the running buffer mentioned above) with varying concentrations of

L-methionine. The second measurement (green curve) is the same as the first experiment, except that N295A E166Q MetNI was used. Both binding curves show biphasic characteristics and are better described by fitting each phase separately (see Materials and Methods, Section 3.4). For both binding curves, the first binding phase was fitted to the Hill equation and the binding affinity was characterized to 7.2 nM; the second phase was fitted as a linear curve on a semi-log scale and is in the range of 100–10 000 nM. The 7.2 nM is assigned as the affinity of MetQ binding L-methionine. The lower affinity in the range of $\sim$ 10 000 nM is thought to be the potential translocation pathway binding L-methionine or the binding of Met to the C2 domain.

Characterization of Intermediate States of the Transport Cycle

Following substrate binding to MetQ, the rest of the transport cycle involves conformational changes from an apo transporter to several intermediates. Since transport is a continuous process, we partitioned it into several major transitions for analysis. For each transition, we characterized the physical characteristics of the transport intermediates. We evoked the characteristics of these species and came up with strategies to stabilize intermediate states with these properties. We then identified biophysical techniques that can best measure the information desired.

We discuss the four, previously-described conformational-states: pre-T, outward, post-T, and inward conformation. Three of these conformations—pre-T, outward, and post-T—are transporter-complexes that have formed a complex with the binding protein. Only the pre-T conformation is bound to a liganded binding-protein. The pre-T state and the outward state are ATP-bound, while the post-T state is ADP- and P_i-bound.

To begin our analysis, we first define the different conformations of the TMDs. The L-methionine binding site formed by the TMDs is called the translocation pathway substrate binding site ('translocation pathway site'). The alternating access model stipulates that there are two major conformations by the opening formed by these two domains and the orientation of the opening with respect to which side of the membrane (Jardetzky, 1966). The outward-facing orientation of the TMDs is such that the domains form a cavity, which opens to the periplasm. The inward-facing TMDs is such that the cavity opens to the cytoplasm. The model further states that the affinity of the translocation pathway site for the substrate is different between the two conformations. It is predicted that when the TMDs are in the outward-

facing orientation, the affinity for the substrate is higher than the inward-facing orientation. The switch to a lower affinity for substrate creates an optimal condition for L-methionine to be dissociated once the translocation pathway site is in the inward-facing conformation.

We constructed a kinetic model (Figure 2.1) that incorporates our analysis and previous experimental observations.

The Pre-Translocation Conformation

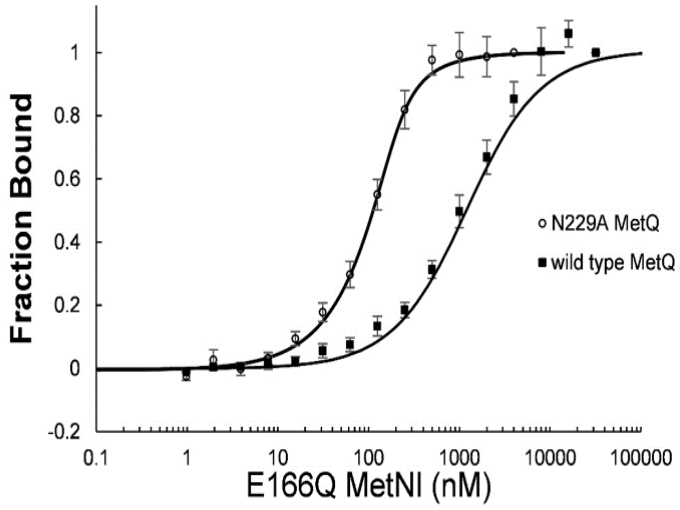

Figure 3.4: **The dissociation constant for liganded- and unliganded-transporter complex** The affinity of MetNI for MetQ was measured by titration curves using fluorescently labeled MetQ—in the presence or absence of bound methionine (wild-type or N229A MetQ, respectively). All experiments contained 1 mM ATP and 1 mM EDTA. 101 nM of Cy3-labeled, wild-type MetQ was titrated with 1.95 nM - 32 μM non-labeled E166Q MetNI (closed squares). 99 nM of Cy3-labeled N229A MetQ was titrated with 1.95 nM - 4 μM non-labeled MetNI E166Q (open circles). The dissociation constants calculated from these data for wild-type (methionine-bound) and N229A (methionine-free) MetQ binding to E166Q MetNI are K_d = (1100 ± 300) nM and (27 ± 9) nM, respectively. Error bars represent standard error from three independent measurements.

The pre-translocation conformation poises the transporter for ATP hydrolysis and substrate translocation. Previous structural work showed that pre-T has semi-open NBDs (Oldham and J. Chen, 2011a). Additionally, the TMDs are predicted to be in the inward-facing orientation (Oldham and J. Chen, 2011a). In our experiment, we showed that ATP is required to form the pre-T state (Figure 3.6). Therefore, the prominent features of this conformation are as follows: TMDs are inward-facing and

bound to a liganded MetQ, and two NBDs are semi-closed. ATP might be bound to either or both halves of the NBDs. In either scenario, since the NBDs are not closed, the transporter is not ready for hydrolysis. We stabilized this conformation under experimentally defined conditions.

First, we showed that ATP is required to stabilize the pre-T state. Since MetNI only has two ATP binding sites in the NBDs, we proposed that either or both sites are occupied by ATP. To probe the pre-T's nucleotide state, we established the MetNI-MetQ complex's SPR profiles under different nucleotide states. Then we compared the stabilized pre-T against each profile and ascertained the nucleotide state of pre-T. This process began by immobilizing unfolded-refolded MetQ. Following the immobilization, we injected E166Q MetNI (solubilized in 0.025% DDM containing 1 mM EDTA) and 1 mM of different nucleotide (ATP, ADP, ADP+Pi, Pi, vanadate, ADP+vanadate, or nucleotide-free) for each measurement onto the flow cells. When we flowed 1000 nM E166Q MetNI over MetQ—in the presence of ATP—we obtained a robust response representing complex formation. Once the injection was terminated (i.e. the washing buffer started), the complex was stable and did not readily dissociate. However, when we flowed 1000 nM E166Q MetNI in the presence of the nucleotides mentioned above, other than ATP over MetQ, no complex formation was observed. This result was observed even when MetNI was in several-fold molar excess of MetQ. This means a complex formation signal in SPR shows that the MetNI-MetQ complex requires ATP.

Previously, we showed that in our SPR setup, L-methionine in MetQ is washed away after the first few measurements. That means we would not be able to stabilize the pre-T state, which has a liganded MetQ. Therefore, we tried to stabilize it in an MST assay. We reasoned that the bound L-methionine would not get dissociated from MetQ in a solution in the absence of a constant flow of MetNI. Use of wild type MetQ—which contains co-purified L-methionine—stabilized the pre-T conformation. L-methionine remained bound to MetQ in solution, versus a constant flow of solution in a Biacore channel, as shown by x-ray crystallography work.

Importantly, we reasoned that a binding protein forms a complex with the transporter at a higher affinity when the TMDs of the transporter are in the outward-facing orientation because there is more surface interaction of the TMDs with the binding protein. Studies in the maltose system suggest that the interaction between liganded binding-protein and the transporter trigger the release of the ATP products ADP and Pi (Bao, Dalal, et al., 2015). It is predicted that MetNI binds to liganded MetQ

first, forming Pre-T. As the MetQ-bound ligand stimulates hydrolysis, the pre-T is promoted to quickly adopt a conformation that is most suitable for hydrolysis (i.e. the outward-facing conformation). Therefore, pre-T converts to the outward facing conformation upon binding ATP. After this isomerization, the complex achieves the highest affinity, which allows hydrolysis and substrate translocation to occur.

We determined the affinity constant for the binding of MetNI to MetQ in this complex to be 1100 nM (Fig. 3.4), which is 40-fold lower than that of the outward conformation (27 nM as measured and discussed in section 3.2). With the observations that complex formation is ATP-dependent, we confirmed the successful stabilization of the pre-T intermediate by the process of elimination. We reasoned that since this state is ATP-required, it can be either pre-T or outward—a post-T transporter is ADP and P_i-bound during hydrolysis. Additionally, we know that the pre-T conformation should bind liganded MetQ, as discussed previously. We verified the pre-T identity with this comparative MST assay (Figure. 3.4).

The Outward-facing Conformation

As previously discussed, L-methionine is bound to MetQ—complexed with MetNI—in the pre-T state. In that state, the translocation pathway site is inward-facing. We propose that the closed L-methionine bound conformation of MetQ triggers the change in conformation of the TMDs from inward to outward. Subsequently, L-methionine dissociates from MetQ and binds to the outward-facing translocation pathway substrate site. In addition to the outward-facing TMDs, the NBDs of MetNI in the outward state are predicted to be closed. Therefore, MetQ is predicted to be open and unliganded in the outward conformation of MetNIQ. The structure of the $MalFGK_2$ outward-facing conformation shows that the substrate is absent from the binding protein (Oldham, Khare, et al., 2007). Additionally, EPR studies show that the two lobes of the binding protein are separated from each other (Austermuhle et al., 2004). Combining these observations, we used unfolded-refolded MetQ to ensure that MetQ is in the open, unliganded state to prepare the outward-facing conformation.

In summary, the essential elements of an outward-facing conformation of an ABC transporter are as follows: (1) the TMDs are open to the periplasm, and hence 'outward-facing'; (2) the NBDs are close to each other and ATP-bound. For ABC importers that are dependent on a binding protein for transport, in the outward state, the transporter is bound to the binding protein. Therefore, the third element is (3)

MetNI is bound to MetQ. (4) During a productive transport, substrate L-methionine should be released to the translocation pathway site. However, it is uncertain whether this fourth element—substrate bound to the translocation pathway site—is necessary to trigger an outward state of the transporter. For instance, structural work on the maltose transporter shows that substrate is bound to the translocation pathway site during the pre-T state. Chen and co-workers concluded that their observation is due to the high concentration of the substrate in the solution (Oldham, S. Chen, and J. Chen, 2013).

We believe the conditions in our SPR experiment (Figure 3.6) trapped a conformation of MetNI that closely resembles the outward state. In this experiment, the trapped conformation of MetNI forms a complex with MetQ and the TMDs are outward-facing; however, there is no substrate bound to any substrate site in the MetNIQ complex. We reasoned that the translocation binding site is trapped in the outward-facing orientation because there is an excess of EDTA that prevents ATP hydrolysis by chelating the Mg^{2+} cofactor. Biophysical data from the Chen group show that when the maltose transporter is in the outward-facing conformation, it is associated with the binding protein and its NBDs are ATP-bound (Orelle, Ayvaz, et al., 2008). Because an association with both ATP and MetQ is essential, we first studied the ATP dependence of the MetNIQ complex to examine the conditions necessary to establish ATP-bound NBDs. We then studied the kinetics of the MetNIQ complex formation.

The molecular events that happen in the outward state are predicted to be coupled so that hydrolysis couples with substrate translocation and the conformational change from outward to post-T. Therefore, ATP must be poised for hydrolysis by being bound to the closed NBDs, a condition necessary *a priori* for all three events mentioned above.

In order to simulate these reactions, we first determined the concentration of ATP required to support complex formation. We measured the concentration of ATP required to get half maximal formation of the MetNIQ complex on the Biacore chip. The concentration was determined to be 50 μM (Figure 3.5) when half of the immobilized MetQ is complexed with MetNI. The ATP-hydrolysis-defective E166Q MetNI mutant was used in combination with saturating concentrations of ATP and EDTA. Consequently, the use of 1 mM ATP ensures that most transporters are ATP-bound.

In addition to ensuring that the NBDs are ATP-bound, we needed to figure out

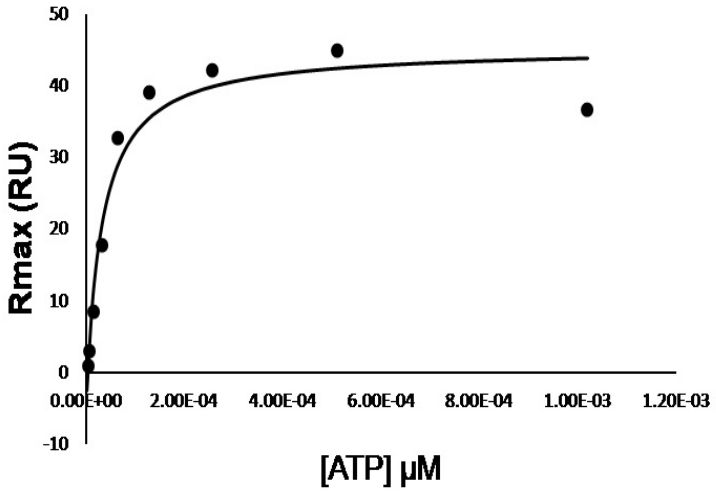

Figure 3.5: **The ATP dependence of the MetNI-MetQ complex formation**. For the assay, the unfolded-refolded MetQ was immobilized on the sensor-chip, Varying concentration (0 - 1 mM) of ATP with a constant concentration of MetNI (1 µM E166Q MetNI solubilized in 0.025% DDM, 20 mM TAPS pH 8.5, 250 mM of NaCl, and 1 mM EDTA was titrated to the immobilized MetQ. It is found that at 50 µM of ATP, half of the MetNI-MetQ complex is ATP-bound.

the conditions that stabilize closed NBDs. There is controversy on the necessary conditions required for the closure of NBDs. In Bao and Duong (2013), the Duong group concluded that NBDs close upon ATP binding. However, in Orelle, Ayvaz, et al. (2008), the Davidson group reasoned that both ATP binding to the NBDs and the transporter interacting with a binding protein are required. Since we already ensured ATP-bound NBDs, we need only establish that binding-protein interactions occur to be certain of stabilized, closed NBDs according to either group's finding.

In detail, as seen in Equation 3.1, this reaction describes apo MetQ, designated as 'Q' in the model, binding to ATP-bound E166Q MetNI, designated by 'ET', to yield 'ETQ'. 'ETQ' then converts to 'ETQ*' . 'ETQ*' is believed to be the conformation before hydrolysis, the outward-facing state. The binding curves in the experiment shown in Figure 3.6 were fitted using the Two State model (see section 3.4 for model description and fitting), which describes a 1:1 binding interaction followed by an isomerization step. k_1 and k_{-1} are the forward and reverse rate constant for MetNIQ complex association and dissociation, respectively. k_2 and k_{-2} are the forward and reverse rate constant for conformational change, respectively.

$$\mathrm{ET} + \mathrm{Q} \underset{k_{-1}}{\overset{k_1}{\rightleftharpoons}} \mathrm{ETQ} \underset{k_{-2}}{\overset{k_2}{\rightleftharpoons}} \mathrm{ETQ}^{*} \tag{3.1}$$

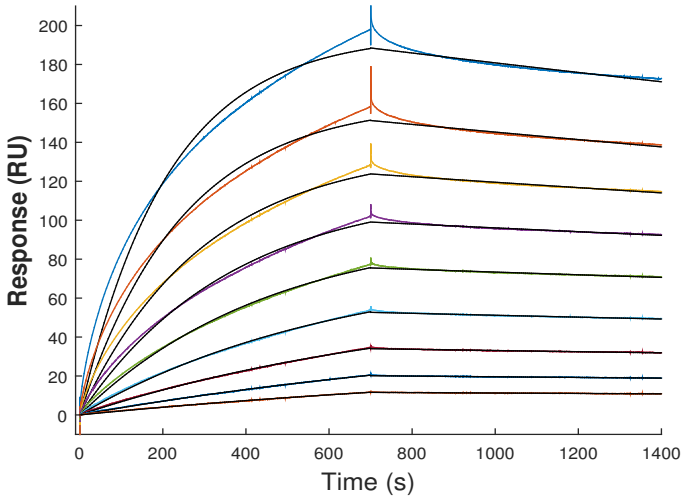

Figure 3.6: **Kinetic Characterization of the outward-facing conformation.** Each colored curve is an experimental binding curve. The binding curves were fitted using the Two State model (see section 3.4 for model description and fitting), which describes a 1:1 binding interaction followed by a isomerization step. k_1 and k_{-1} is the forward and reverse rate constant for complex association and dissociation, respectively. k_2 and k_{-2} are the forward and reverse rate constant for conformational change, respectively. The k_1 is 5.6×10^3 M^{-1} s^{-1}, k_{-1} is 7.4×10^{-5} s^{-1}, k_2 is 1.7×10^{-3} s^{-1}, k_{-2} is 1.2×10^{-2} s^{-1}, and K_d is 1.1×10^{-8} M. In this assay, the unfolded-refolded MetQ was immobilized on a sensor-chip. The chip was then equilibrated with a running buffer: (25 mM TAPS, pH 8.5, 250 mM NaCl, 0.025% DDM, 1 mM ATP, 1 mM EDTA). E166Q MetNI (Lm construct) of varying concentrations (range from 1 to 1000 nM) was injected to interact with MetQ in a time-, and speed-controlled manner. After each injection, a glycine solution of pH 2 was used to wash off the bound E166Q MetNI. MetQ was tested to be stable under this washing condition.

$$K_d = \frac{k_{-1}}{k_1} \times \frac{k_{-2}}{k_{-2} + k_2} \tag{3.2}$$

The association and dissociation curves showed biphasic characteristics, as expected, to reflect an isomerization step following the binding step (Figure 3.6). Therefore, we fitted the data to a two-state model to account for these results. Under the experimental conditions, E166Q MetNI forms a complex with apo MetQ with a k_1 of 5.6×10^3 M^{-1} s^{-1}, k_{-1} is 7.4×10^{-5} s^{-1}, k_2 is 1.7×10^{-3} s^{-1}, k_{-2} is 1.2×10^{-2} s^{-1} and K_d is 1.1×10^{-8} M according Equation 3.2. k_1 and k_{-1} are the forward and reverse kinetic rate constants for complex formation and dissociation, respectively. k_2 and k_{-2} are the forward and reverse rate constant for conformational change, respectively. The Biacore binding assay showed that the outward-facing conformation

SPR	k_1	k_{-1}	k_2	k_{-2}	K_d
Unit	$\text{M}^{-1}\,\text{s}^{-1}$	s^{-1}	s^{-1}	s^{-1}	M
Constants	5.6×10^3	7.4×10^{-5}	1.7×10^{-3}	1.2×10^{-2}	1.1×10^{-8}

Table 3.2: **The kinetic constants of the outward-facing state using SPR** According to the two-state model, k_1 and k_{-1} are the forward and reverse rate constant for MetNI-MetQ complex formation, respectively. k_2 and k_{-2} are the forward and reverse rate constant for an isomerization step, respectively. K_d is the dissociation constant for MetNI and MetQ forming MetNI-MetQ according to the Equation 3.2.

MST	K_d
Constants	2.7×10^{-8} M

Table 3.3: **The dissociation constant of the outward-facing state using MST.** This measurement is from the experiment shown in Figure 3.2

has a higher affinity than all other known Type I importer transporter-complexes (Table 2.1). Also, the affinity of the outward state measured by SPR is similar to the value measured by MST (Figure 3.3).

The Post-translocation State: Post-hydrolysis reaction simulation

SPR	k_1	k_{-1}	k_2	k_{-2}	K_d
Unit	$\text{M}^{-1}\,\text{s}^{-1}$	s^{-1}	s^{-1}	s^{-1}	M
Constants	$9.8 \times 10^3\ \text{M}^{-1}\,\text{s}^{-1}$	$9.1 \times 10^{-4}\ \text{s}^{-1}$	$3.3 \times 10^{-6}\ \text{s}^{-1}$	$9.5 \times 10^{-3}\ \text{s}^{-1}$	9.3×10^{-8} M

Table 3.4: **Nucleotide can exchange without the dissociation of binding protein.** According to the two-state model, k_1 and k_{-1} are the forward and reverse rate constant for MetNI-MetQ complex formation, respectively. k_2 and k_{-2} are the forward and reverse rate constant for an isomerization step, respectively. K_d is the dissociation constant for MetNI and MetQ forming MetNI-MetQ according to the Equation 3.3.

After translocation has occurred, MetQ must dissociate to reset the transporter. MetQ dissociation is facilitated by the release of the ATP hydrolysis products. To stabilize the post-T state, we must ensure the transporter is still MetQ-bound and the hydrolysis-products are still intact. We learned to stabilize the post-T conformation by recalling results from the maltose transporter. In these transporters, the vanadate-stabilized, post-translocation state is formed by trapping the products of hydrolysis

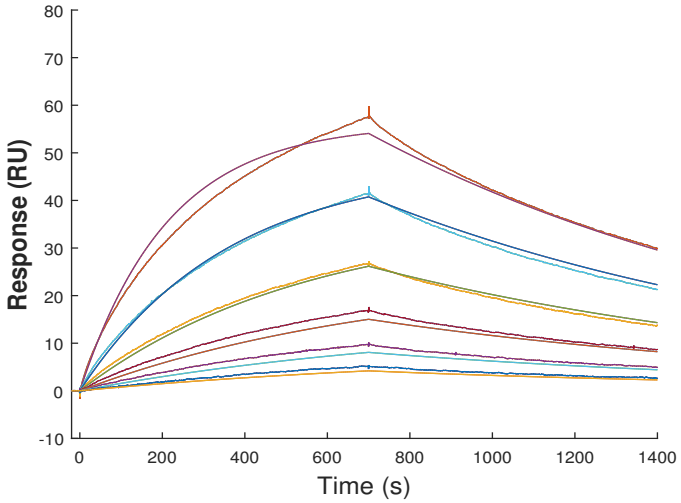

Figure 3.7: **Mg^{2+} stimulates ATP hydrolysis.** Each colored curve is an experimental binding curve. In this assay, the unfolded-refolded MetQ was immobilized on a sensor-chip. The chip was then equilibrated with a running buffer: (0.025% DDM, 25 mM TAPS, pH 8.5, 250 mM NaCl, 1 mM ATP, 1 mM Mg^{2+}). E166Q MetNI (Lm construct) of varying concentrations (range from 1 to 1000 nM) was injected to interact with MetQ in a time-, and speed-controlled manner. After each injection, a glycine solution of pH 2 was used to wash off the bound E166Q MetNI. MetQ was tested to be stable under this washing condition.

in the NBDs (Sharma and Davidson, 2000). Other conditions that attempt to recreate this trapped complex, such as adding ADP only, vanadate only, or ADP and vanadate were unsuccessful. That means, the post-T must be trapped right after hydrolysis and before ADP and Pi are released; adding the products of hydrolysis after the original ADP and P_i have been released does not recreate the post-T state.

We learned that the basal rate of hydrolysis in mutant E166Q MetNI can be stimulated by the addition of Mg^{2+}. Therefore, our experiment (Figure 3.7), which aims to trap the MetNI post-T state, involves E166Q MetNI binding to MetQ in the presence of ATP and Mg^{2+}. In this experiment, both ATP and Mg^{2+} are present in the running buffer. That means after each cycle of hydrolysis, the hydrolysis products (i.e. ADP and Pi) can be replaced by the ATP in the solution. Here, we have a pool that contains a mix of ATP- and ADP+Pi-bound transporters. This complex has an affinity of 9.3×10^{-8} M (Table 3.4).

It is hypothesized that the hydrolysis defective transporter slows the release of ADP and P_i, hence stabilizing the post-T state. Another piece of supporting evidence is that the lack of bound substrate in the binding protein makes the release of P_i

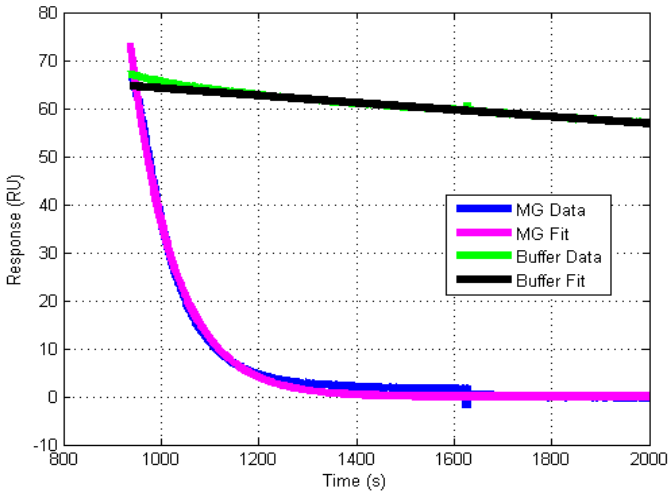

Figure 3.8: **ATP hydrolysis stimulates MetQ dissociation.** The rate constant of dissociation of the complex MetNIQ when hydrolysis is minimized is $1.2 \times 10^{-4}\,s^{-1}$. The rate constant of dissociation when hydrolysis is stimulated by Mg^{2+} is $1.1 \times 10^{-2}\,s^{-1}$. MetQ dissociates slowly from the MetNIQ complex in the presence of ATP and EDTA (green binding curve). If EDTA and ATP were removed and Mg^{2+} was introduced, the dissociation is accelerated (blue binding curve). The black and magenta curve are the fits according to the single exponential decay function to the experiments mentioned above, respectively. In this assay, the unfolded-refolded MetQ was immobilized on a sensor-chip. For the green binding curve, 1 µM E166Q MetNI (Lm construct) solubilized in (0.025% DDM, 25 mM TAPS, pH 8.5, 250 mM NaCl, 1 mM ATP, 1 mM EDTA) was flowing in the channel to interact with the immobilized MetQ. For the blue binding curve, the same setup, construct, and buffer condition was used, except EDTA and ATP was taken out and Mg^{2+} was added.

rate-limiting (Bao, Dalal, et al., 2015). As such, we have reason to believe that some products of hydrolysis are retained within the complex. The fact that we still observed signals for complex indicates that we have trapped the post-T. The affinity of the post-T state is roughly one order of magnitude lower than the outward state, which is 1.1×10^{-8} M as seen in Table 3.2.

To further understand events after translocation, we designed an experiment (shown in Figure 3.8) where there is no replacement of ATP after hydrolysis. In this experiment, the green and the black curves are the buffers containing ATP and EDTA. The blue and magenta curves show the destabilization of the MetNI-Q complex stimulated by Mg^{2+} when there is no ATP for replacement in the buffer. The rate constant of dissociation when hydrolysis is stimulated by Mg^{2+} is $1.1 \times 10^{-2}\,s^{-1}$. Since the rate constant of dissociation is the element that changes with the addition

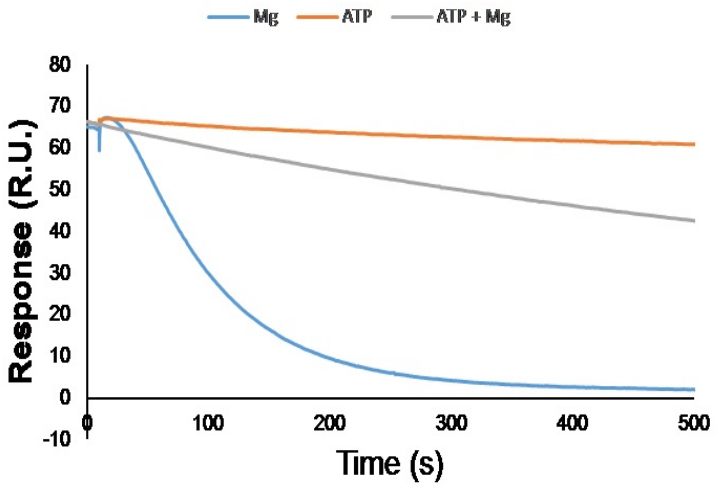

Figure 3.9: **ATP can be replaced while the binding protein is bound to the transporter.** Here, a comparison of the dissociation phase of the MetNIQ complex under three conditions: ATP, Mg^{2+}, and ATP+Mg^{2+}. With ATP, the complex dissociates minimally. With ATP and Mg^{2+}, the dissociation rate constant is faster; and much faster with Mg^{2+} alone.

of Mg^{2+}, this rate presumably reflects the rate of ATP hydrolysis.

Lastly, we compared the kinetics of the MetNIQ complex under three different conditions in Figure 3.9. Under the condition of ATP+EDTA, which minimizes hydrolysis; ATP+Mg^{2+}, which stimulates hydrolysis and the products of hydrolysis can be replaced by the ATP in the buffer; Mg^{2+}, which stimulates hydrolysis, however, the products of hydrolysis are still bound within the NBDs. We observed that hydrolysis with replacement of ATP destabilized the complex, while hydrolysis with no ATP replacement further destabilized the complex in comparison.

$$ETQ^{*} \rightleftharpoons EDQ \rightarrow ED + Q \tag{3.3}$$

The Inward-facing conformation

After substrate translocation, a series of events occur that are important to establishing the resting state: the inward-facing conformation. The following observations increased our understanding of the sequence of events that happened post-translocation. First, hydrolysis stimulated the opening of the NBD (Moody et al., 2002); this is in agreement with the fact that the inward-facing state crystal structure of MetNI exhibits open NBDs. Second, our SPR studies showed that

hydrolysis prompts the dissociation of MetQ from MetNI (Figure 3.7). Based on these observations, the sequence of events that occur is predicted to be as follows: a liganded MetQ interacts with the transporter to trigger hydrolysis as discussed in Section 3.2. Hydrolysis then resets the ATP-binding cassette dimer into the resting-state conformation through the separation of the NBDs (G. Lu et al., 2005). Subsequently, the opening of the NBDs prompts the releases of ADP and Pi. Following the release of these nucleotides, MetQ dissociates, prompting the transporter to adopt the inward-facing conformation, with open, nucleotide-free NBDs.

There are two fates of the inward-facing conformation. One route occurs when the intracellular concentration of L-methionine is high; L-methionine binds to the C2 domain of MetNI and stabilizes the transporter in the inward-facing state. L-methionine bound inward-facing MetNI is called the inhibition state. The other fate is when ATP binds to the transporter and forms 'ET', which after binding MetQ will start a new transport cycle.

The Inhibition State

Unique to the MetNI system, L-methionine binds the C2 domain of MetNI and stabilizes the inward-facing state. This is believed to be the molecular cause for the phenomenon of trans-inhibition (Kadaba et al., 2008; Yang and Rees, 2015). The effect of L-methionine binding to the complex was investigated through a BiaCore experiment with mutant N229A MetQ (mutant contributed by P. Nguyen), which significantly compromises the capacity of MetQ to bind L-methionine, which allows us to examine the effect of L-methionine binding the C2 domain. We immobilized the N229A MetQ on a sensor chip, and a binding curve was generated when varying concentrations of L-methionine was titrated—each titrant consists a constant concentration (1 μM) of E166Q MetNI solubilized in 0.025% DDM, 25 mM TAPS pH 8.5, 250 mM NaCl, 1 mM ATP, and 1 mM EDTA. The binding curve fit a 1:1 model (Fig. 3.10) and yielded a K_d of 220 μM, compared to 30 μM in a separate ATPase activity measurement (Yang and Rees, 2015).

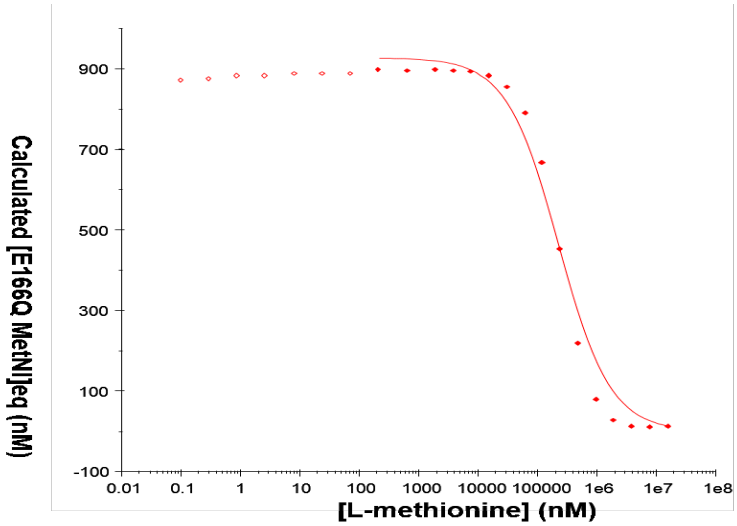

Figure 3.10: **K_d for L-methionine binding to the C2 domain of MetNI is 2.2×10^{-4} M.** To measure the binding capacity of the C2 domain to L-methionine, the mutant N229A MetQ was immobilized on the sensor-chip. Varying concentrations of L-methionine (100 pM to 16 mM) were titrated to the sensor chip. Each titrant has a constant concentration of the Lm construct of E166Q MetNI (1 µM) solubilized in 25 mM TAPS pH 8.5, 250 mM NaCl, 0.025% DDM, 1 mM ATP, and 1 mM EDTA. The results are plotted with the y-axis as the reported concentration of MetNI complex; x-axis as [L-methionine]. The binding curve fits to the one to one binding model and yielded a K_d of 2.2×10^{-4} M. There is an observation of cooperativity in the fit.

3.3 Discussion

We characterized the kinetics and affinities of the major transporter conformations of MetNI during the transport cycle. These conformations are: the pre-translocation, outward-facing, post-translocation, inward-facing, and inhibition state. Using these measurements, along with previously reported structural information, we developed a quantitative transport-framework (Figure 3.11).

According to this model, apo-, unliganded-MetNI readily binds ATP to form 'ET'. 'ET' is predicted to bind to a closed, liganded MetQ; this interaction results in the pre-translocation state. The pre-T has an affinity of 1.1×10^{-6} M. When L-methionine moves to the translocation pathway, the transporter adopts the outward conformation. We trapped the outward by allowing a complex to be formed between apo MetQ and ATP-bound E166Q MetNI. We believed that the trapped outward had undergone a conformational change—upon MetNI binding to MetQ—to achieve a high affinity complex. This two-step reaction is fitted to the two-state model. The forward and reverse rate constant for complex formation are 5.6×10^3 M^{-1} s^{-1}

	ETQ	ETQ*				EDQ	ED + Q
	Pre-T	Outward				Post-T	Inward
MetQ	closed, liganded	open				open	not bound
TMDs	inward	outward				inward	inward
NBDs	ATP, semi-open	ATP, closed				ADP-Pi, semi-open	free, open
Technique	MST	MST	SPR			SPR	N/A
Constants	K_d	K_d	k_1	k_{-1}	K_d	$k_{dissociation}$	N/A
Unit	M	M	$M^{-1}\,s^{-1}$	s^{-1}	M	s^{-1}	N/A
Constants	1.1×10^{-6}	2.7×10^{-8}	5.6×10^{3}	7.4×10^{-5}	1.1×10^{-8}	1.1×10^{-2}	No Complex
	Fig. 3.4	Fig. 3.4	Fig. 3.6			Fig. 3.8	N/A

Table 3.5: **A summary of the kinetic constants of different conformations for MetNI.** The major conformations include pre-T, outward, post-T, and inward conformation. All of these conformations have been characterized kinetically and thermodynamically by biophysical techniques i.e. SPR and MST. k_1 is and k_{-1} is for the forward and reserve rate constant for MetNI-MetQ complex formation, respectively. k_2 and k_2 is the forward and reverse rate constant for an isomerization step, respectively. K_d is the dissociation constant for MetNI and MetQ forming MetNI-MetQ.

and $7.4 \times 10^{-5}\,s^{-1}$, respectively. The forward and reverse rate constant for the isomerization are $1.7 \times 10^{-3}\,s^{-1}$ and $1.2 \times 10^{-2}\,s^{-1}$, respectively. The K_d is fitted to be 1.1×10^{-8} M. This affinity similar to the value measured with MST (K_d = 2.7×10^{-8} M; Figure 3.4). The conformational change from pre-T to outward is concomitant to the substrate dissociates from MetQ, and binds to the translocation pathway site. Therefore, the outward is in association with an open, unliganded MetQ. Also, it has closed, ATP-bound NBDs that are ready for hydrolysis.

While the substrate remains in the translocation pathway site, a conformational change from the outward to the post-T occurs turning the substrate to the cytoplasm as the two TMDs open up towards the inside of the cell. Hydrolysis occurs concomitant to substrate translocation. Since hydrolysis stimulates the dissociation of MetQ from MetNI, the transporter returns to the inward-facing state, which is inactive for substrate transport and hydrolysis. There are two fates to the inward-facing intermediate. If the concentration of ATP is high, most of the transporter is ATP-bound, which means most of the transporters are in the 'ET' state. Otherwise, if the L-methionine concentration is high relative to ATP, both L-methionine and ATP can bind to the transporter. As long as L-methionine is bound to the C2 domain, the

transporter adopts an inhibition state, which is inactive for transport.

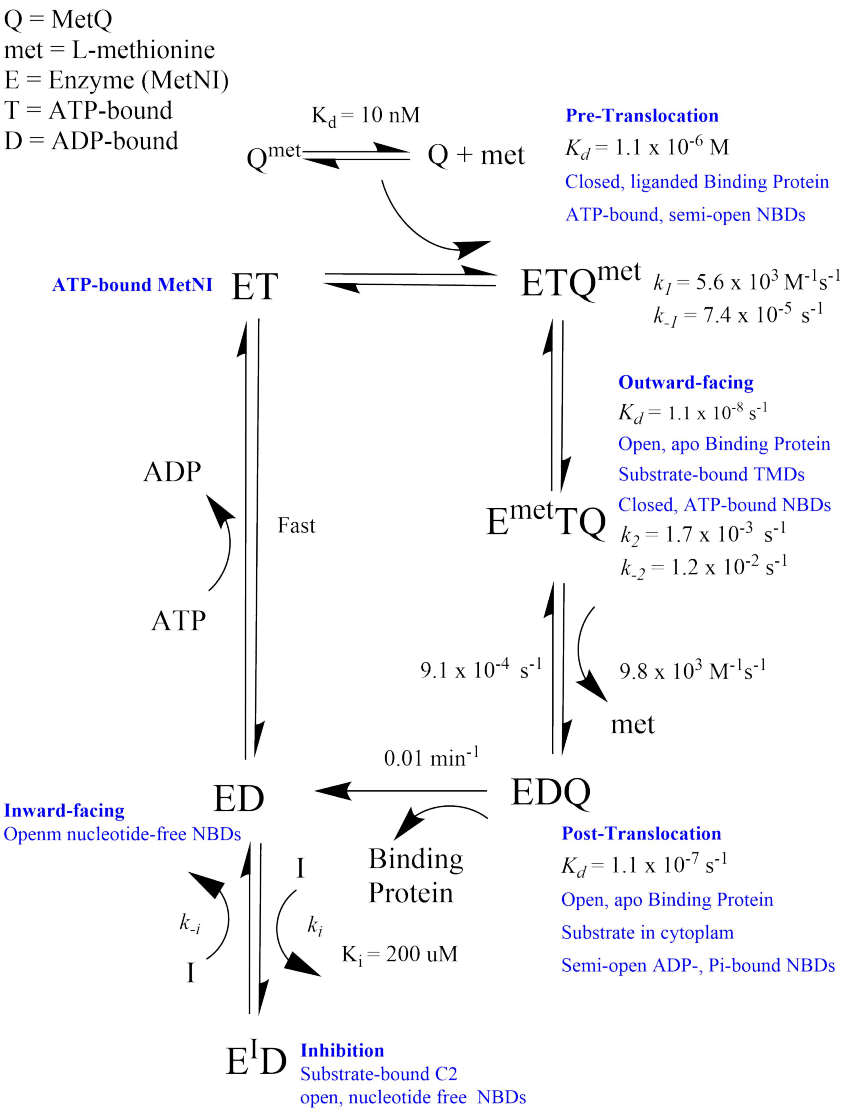

Figure 3.11: **Thermodynamics of the MetNI-Q transport cycle.** This model proposes six intermediates during the transport cycle, with four of the six states as complexes. An additional conformation, E^ID is included in the trans-inhibition step. During this step, the intracellular concentration of L-methionine as an inhibitor (I) is high, I binds to ED to inhibit ATP hydrolysis. The model predicts that E^ID, the enzyme-inhibitor complex, will not be released by the addition of substrate, but instead by the decreased concentration of the inhibitor.

3.4 Materials and Methods

Cloning, expression, and purification of MetQ

The *MetNIQ* operon was amplified from *Escherichia coli* K-12 genomic DNA and cloned into a zero blunt pCR-4 TOPO vector as described in (Kadaba et al., 2008). The *MetQ* gene, lacking the stop codon, was subcloned using oligonucleotides that included *NdeI* and *XhoI* restriction-enzyme sites, and then ligated into the pET21b(+) vector with a C-terminal 6x-histidine tag. The cloned plasmids were expressed separately in *E. coli* BL21 (DE3) gold cells (EMD) at 37 °C in Terrific Broth medium with 100 µg mL^{-1} ampicillin. The cells were induced at OD600 ~ 4.0 with 0.4 mM IPTG for 2 h, then harvested and stored at −80 °C.

For purification of mature MetQ, periplasmic extract was prepared by re-suspending 10 g of cell paste in 10 ml of 40% sucrose, 10 mM Tris-HCl pH 7.5, and 1 mM EDTA, and stirred for one hour at room temperature. The cells were then shocked by addition of 500 ml of ice-cold water. After stirring for 10 min, buffer components were added to a final concentration of 25 mM Tris pH 7.5, 150 mM NaCl, and 17 mM imidazole. The resulting suspension was then centrifuged at 37,500 x g for 30 min to remove all cellular debris from the periplasmic extract. MetQ was isolated from the periplasmic extract by immobilized metal ion affinity chromatography using a 5 ml Ni-NTA column (GE). The affinity column was washed with 25 mM Tris pH 7.5, 150 mM NaCl, and 17 mM imidazole for 10 column volumes. Protein was then eluted from the column using 25 mM Tris pH 7.5, 100 mM NaCl and 150 mM imidazole. Peak fractions were dialyzed against 25 mM Tris pH 7.5 and 150 mM NaCl overnight, and then concentrated to 30 mg/ml using a 10kD MWCO concentrator (Millipore).

The full-length MetQ protein cloned for this work, including the signal sequence and the C-terminal 6x-his tag, has the sequence:

MAFKFKTFAAVGALIGSLALVGCGQDEKDPNHIKVGVIVGAEQQVAEVAQ
KVAKDKYGLDVELVTFNDYVLPNEALSKGDIDANAFQHKPYLDQQLKDRG
YKLVAVGNTFVYPIAGYSKKIKSLDELQDGSQVAVPNDPTNLGRSLLLLQKV
GLIKLKDGVGLLPTVLDVVENPKNLKIVELEAPQLPRSLDDAQIALAVINTTY
ASQIGLTPAKDGIFVEDKESPYVNLIVTREDNKDAENVKKFVQAYQSDEVY
EAANKVFNGGAVKGWLEHHHHHH

The cleaved signal sequence is highlighted in bold, so that the purified protein used in this study consists of residues 17 to 279, of which residues 29-273 (underlined) are observed in the electron density.

Unfold and refold MetQ to get rid of co-purified L-methionine

We also learned from the structural studies (Johnson et al., 2012) that MetQ in the absence of substrate would give the highest affinity. Therefore, the purification of the MetQ has undergone an unfolded (with high concentration of guanidinium HCl) and a refolded step to eliminate co-purifying methionine.

Post cell lysis (Section 3.4), supernatant was separated from the cell pellet via ultra-centrifugation. The supernatant was then loaded onto an affinity chromotagraphy column. The loaded MetQ goes though washed with the Purification buffer, then an unfolding step with the Unfolding buffer, another wash step, and then was eluted with the Elution buffer. Buffer conditions are listed below.

Purification buffer (25mM Tris-HCl pH7.5, 150mM NaCl) and Elution buffer (25mM Tris-HCl pH7.5, 150mM NaCl, 1M Imidazole). The unfolding buffer (6 M Guanidine-HCl, 25 mM Tris-HCl pH7.5, 150 mM NaCl, 1mM BMe). The refolding buffer (25mM Tris-HCl pH7.5 , 150mM NaCl).

Purification of MetNI

Purification of wild-type and mutant E166Q MetNI was carried out as described (Johnson, Nguyen et al. 2012) with the one modification that buffer containing 20 mM TAPS pH 8.5, 100 mM NaCl and 0.025% DDM (with varying amounts of imidazole) was used in all purification steps (the original protocol used 250 mM NaCl and different detergents).

SPR Assay

The Lo construct of MetQ was overexpressed, purified, unfolded and then refolded using 6 M guanidine hydrochloride. MetQ was then immobilized on a CM5 (carboxymethyl dextran) chip (GE Healthcare, BR-1005-30) gold surface via EDC-NHS activated carboxylate groups. 1 µg/mL of MetQ was concentrated to the surface with pH 4.5 acetate (the p.I. of MetQ is 5.63 (ExPASy Estimate)) to achieve a signal of 100 RU. Excess MetQ on the surface was washed off using a 50 mM NaOH solution. The carboxyl groups on the sensor-chip are activated to provide the reactive succinimide esters with the addition of a mixture of NHS (N-hydroxysulfosuccinimide) and EDC (1-ethyl-3-(3-dimethylaminopropyl) carbodiimide hydrochloride). The primary amine groups on MetQ can bind to these active esters readily to form an amide bond. Upon binding of MetQ to the dextrin, the unbound reactive groups on the surface were deactivated with the addition of ethanolamine. The running buffer

for immobilization is HBS-EP+.

BtuF, the binding protein for the Vitamin B12 transport system was immobilized in the control cell. BtuF has a similar mass to MetQ and BtuF is also an ABC transporter binding protein. Therefore, it makes it a good choice for a control. The use of BtuF is to preclude any non-specific binding to the chip or other random proteins. MetNI was introduced into the microfluidic system by suction. The addition of MetNI to MetQ is speed-controlled and the signal over time of start injection to the end is recorded. The sensor-chip is equilibrated and normalized before the first injection of the MetNI, and subsequently takes real-time pre-steady state measurement of MetNI binding to MetQ. The refraction index change when matter is introduced to the system is subtracted from the binding curve. The curve is also normalized with respect to the control flow cell.

In theory, either MetNI or MetQ can be the ligand (to be immobilized on the sensor chip). However, there has been no success immobilizing MetNI, either is via amine chemistry, Antibody capture, or Ni-NTA capture. With the former two, there is no binding response. With the latter, there is constant a decrease of the signal meaning the ligand keeps falling off of the NTA tethering.

The only successful immobilization is through a EDC/NHS target towards primary amines in MetQ. MetNI serves as the analyte. Although this immobilization configuration is non-specific, measurement is consistent and reproducible each time. It is predicted some primary amines are more exposed than others and the immobilization ended up specific.

The MetQ-immobilized sensor-chip was then equilibrated with the assay running buffer (25 mM TAPS, pH 8.5, 250 mM NaCl, 0.025% DDM, 1 mM ATP, 1 mM EDTA). E166Q MetNI (Lm construct) of varying concentrations (range from 1 to 1000 nM) was injected to interact with MetQ in a time-, and speed-controlled manner. After each injection, a glycine solution of pH 2.0 was used to wash off the bound E166Q MetNI. MetQ was tested to be stable under this washing condition.

For MetNI titration against, MetQ-ATP, varying concentrations (ranging from 16.5 nM to 1000 nM) of E166Q MetNI were added (one concentration per cycle). The binding curves were fitted (See Figure SPR.1) to a 1:1 model that describes one analyte binds to one ligand. k_1 of 1600 $M^{-1}s^{-1}$ and k^{-1} of 9.95 $\times 10^{-5} s^{-1}$ were obtained.

For ATP titration against MetNIQ, a constant concentration (1024 nM) of E166Q

MetNI (20 mM, TAPS, pH 8.5, 250 mM NaCl, 0.025% DDM, 1 mM EDTA) was titrating against different concentrations (1 mM, 300 210 μM, 50 210 μM, 20 210 μM) of ATP (Figure. SPR.2). The R_+max is plotted against the concentration of ATP and a K_d of 50 210 μM is obtained.

ATP Titration on E166Q MetNI and both MetQ (N229A and wild-type) 50 nM wild-type MetQ (Lf construct) was labeled with Cy3 with 40% labeling efficiency and 1 210 μM of E166Q MetNI, were titrated against varying concentrations of ATP (ranging from 0.5 210 μM to 512 210 μM). An EC50 of 25.1 ± 0.525 μ M and a hill coefficient of 1.6 ± 0.0335 210 μM was obtained. If n is fixed to 2, an EC50 of 24.4 ± 0.595 was obtained.

Data Analysis

Data analysis started with establishing the model of the molecular interaction. Common models include 1:1; two-state, bivalent, etc. The prediction of which model would fit the data best can be derived from the prior experimental data. Here we describe the derivation of a 1 : 1 model. More complex models can be derived following the same procedure.

The 1:1 model, which describes one molecule, A binds to one molecule, B to form complex AB. Because of available biophysical data on ABC type I transporters, we are confident that this model is accurate in that one MetQ binds to one MetNI.

The method to deduce the rate of ATP hydrolysis will be discussed. The rate of ATP hydrolysis was assumed to indirectly correlate to the rate of dissociation. In the case of dissociation being the limited rate, then the measured rate is still the rate of dissociation.

R_{max} is the analyte binding capacity of the surface (RU). It is obtained by fitting binding data to a model. Below we show derivation for a 1:1 binding model according to Equation 3.4.

A = MetQ

B = MetNI

$$A + B = AB \tag{3.4}$$

These are the relationships that are true:

$$[A]_{max} \approx R_{max} \tag{3.5}$$

[B] is constant

$$[\mathrm{A}] = [\mathrm{A}]_{\max} - [\mathrm{AB}] \tag{3.6}$$

$$[\mathrm{AB}] \approx \mathrm{R} \tag{3.7}$$

$$K_d = \frac{k_{-1}}{k_1} \tag{3.8}$$

$$\frac{d[\mathrm{AB}]}{dt} = k_1[\mathrm{A}][\mathrm{B}] - k_{-1}[\mathrm{AB}] \tag{3.9}$$

$$\frac{d[\mathrm{R}]}{dt} = k_1(\mathrm{R}_{\max} - [\mathrm{AB}])[\mathrm{B}] - k_{-1}[\mathrm{AB}] \tag{3.10}$$

$$\frac{d[\mathrm{R}]}{dt} = k_1(\mathrm{R}_{\max} - R)[\mathrm{B}] - k_{-1}R \tag{3.11}$$

Solve the differential equation for R:

$$R = \frac{\mathrm{R}_{\max}[\mathrm{B}]}{K_d + [\mathrm{B}]}(1 - \frac{1}{exp^(k_1[\mathrm{B}] + k_{-1})t}) \tag{3.12}$$

Aggregate the constants together for fewer constant terms:

$$R = C_1(1 - exp(-C_2t)) \tag{3.13}$$

Using Eq. 3.13 to fit the SPR binding data. The fit will output C_1 and C_2. The goodness of the fit can be evaluated using graphing the residuals between the data and the fit as well as chi square.

$$C_1 = \frac{\mathrm{R}_{\max}[\mathrm{B}]}{Kd + [\mathrm{B}]} \tag{3.14}$$

$$C_2 = k_1[\mathrm{B}] + k_{-1} \tag{3.15}$$

The same approach is taken to established relationship between kinetic constants with concentration of binding partners the Two State model (Equation 3.17). The equation for the two State reaction is:

$$A + B = AB = AB* \tag{3.16}$$

k_1 is the association rate constant for analyte binding, in the unit of($M^{-1}s^{-1}$).

k_{-1} is the dissociation rate constant for analyte from the complex, in the unit of s^{-1}.

k_2 is the forward rate constant for the conformational change, in unit of s^{-1}.

k_{-2} is the reverse rate constant for the conformational change, in unit of s^{-1}.

All four parameters are obtained from fitting the binding data to the Two Model state.

$$K_d = \frac{k_{-1}}{k_1} \times \frac{k_{-2}}{k_{-2} + k_2} \tag{3.17}$$

Sometimes it is possible to deduce other information than kinetics of molecular binding. An example of this would be the rate of ATP hydrolysis. Once a ATPase defective mutant of the MetNI transporter in the presence of EDTA; separately with Mg^{2+}. In comparison, one can calculate the rate of stimulated hydrolysis by magnesium.

MST Assay

The *E. coli* MetQ sequence contains one cysteine residue at amino acid position 23. Purified wild-type MetQ and N229A MetQ were labeled with Cy3-maleimide (GE Healthcare), according to the manufacturer's instructions, in buffer containing 25 mM Tris pH 7.5, 150 mM NaCl, and 10 mM TCEP pH 7.5. Unreacted dye was removed using a Superdex 200 10/300 GL column (GE Healthcare) equilibrated with the aforementioned buffer condition. The label to protein ratio was determined using a NanoDrop 2000 Spectrophotometer (Thermo Scientific) at 550 and 280 nm, and a labeling efficiency of 10% was calculated. Fluorescence measurements were performed on a Monolith NT.115 Instrument (NanoTemper Technologies GmbH) at 25 °C using standard capillaries. Varying concentrations (ranging from 1.95 nM to 32 µM) of unlabeled E166Q MetNI in ATP buffer (1 mM ATP, 1 mM EDTA, 20 mM TAPS pH 8.5, 100 mM NaCl, and 0.3 % Cymal-5) were titrated against a constant concentration of MetQ (101 nM of wild-type MetQ or 99 nM of N229A MetQ).

Fluorescent intensity as a function of E166Q MetNI concentration was normalized to fraction bound by averaging the intensity values for the lowest three concentrations of E166Q MetNI per experiment. This background intensity was subtracted from all concentrations to yield corrected intensity values. The corrected intensity values were then divided by the corrected intensity at the highest concentration of E166Q MetNI to normalize intensity values to fraction bound values. Dissociation constants for wild-type MetQ or N229A MetQ binding to E166Q MetNI were calculated using the K_d Fit function of the NanoTemper Analysis 1.5.41 software. Three independent MST measurements per condition were conducted, and error bars represent standard error of the mean.

Substrate Binding Sites Measurement

A calibration curve was generated by titrating varying concentrations of E166Q MetNI solubilized in 1 mM ATP containing buffer (25 mM TAPS, pH 8.5, 250 mM NaCl, 0.025% DDM, 1 mM ATP, 1 mM EDTA). Upon calibration, using the same buffer. MetQ was immobilized via a covalent bond to carboxymethylated dextran CM5 sensor-chip within the microfluidic channels for the Biacore system while MetNI was flowing through the volume in the channels. Since L-methionine has an inhibitory effect on the stability of the complex MetNI-MetQ, as L-methionine binds to each binding site on the complex, more complex is destabilized and this change can be detected by SPR. To do this measurement, both proteins MetNI and MetQ are kept at a constant concentration, the concentration of L-methionine varies. Binding information of L-methionine can be extrapolated depending on the cooperativity of the binding sites.

3.5 Supplemental Materials

Evaluation methods for SPR binding data fitting

The SPR binding curves are fitting based on different models that are appropriate for the different reactions. How good are the fits? Primarily, we have two ways of evaluating the fits: the residual graph and the Chi-squared test.

The residual graph

The residual of a fitted binding curve is described by Equation 3.18. For example, we plotted out the residual for an experiment in Chapter 3 (Figure 3.6). As seen in Figure 3.12, we can see that the highest concentration of MetNI (the blue curve) fits the least. The fit becomes better gradually as the protein concentration decreases. This tread might be due to the artefacts that arise when the protein concentration is too high.

$$residual = data - fit \tag{3.18}$$

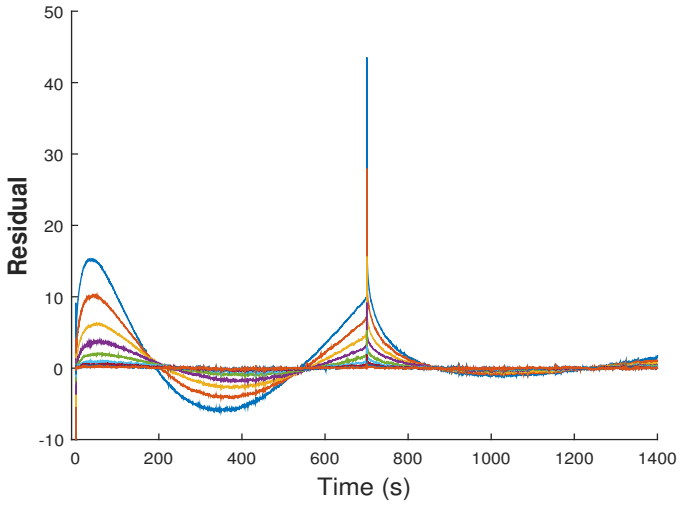

Figure 3.12: Residual analysis for the fit for the data from the SPR experiment with ATP and EDTA.

The residuals show that the fit was better for titration of lower MetNI concentration as the residuals decrease towards the end of the table. This is consistent with the visual inspection of Fig. 3.6. The residual for k_{-1} are very small and the same. It reflects the almost identical dissociation curves.

Residuals	-	8192 nM	4096 nM	2048 nM	1024 nM	512 nM	256 nM	128 nM	64 nM	32 nM
for k_1	10^3	4.7	4.1	2.1	3.4	2.8	2.2	1.6	1.2	0.8
for k_{-1}	10^{-4}	1	1	1	1	1	1	1	1	1

Table 3.6: Residuals for the data and the fit as a metric to evaluate the quality of the fit. Calculation was done with MATLAB.

[MetNI]	8192 nM	4096 nM	2048 nM	1024 nM	512 nM	256 nM	128 nM	64 nM	32 nM
chi^2	0.02	0.02	0.028	0.03	0.039	0.048	0.06	0.079	0.1

Table 3.7: Chi square calculation for the data fitting.

Chapter 4

CONCLUSION

The framework for understanding conformational changes coupled to substrate translocation for ABC transporters started with the Alternating Access Model in 1966. Through four decades of structural determination of ABC transporters, there have been four significant conformations (pre-translocation, Outward-facing, post-translocation, and inward-facing) identified to be pivotal for transport. My interest has been to characterize the E. coli MetNI methionine ABC transporter that was first identified in the 1970s.

We placed an emphasis on kinetic and equilibrium measurements and a focus on understanding conformational changes of the transporter during the transport cycle to complement pre-existing structural knowledge. We quantified the nature of the different conformations for the MetNI system. We also characterized the binding affinity of the substrate binding sites. We added rate and affinity information for each major conformation to the proposed kinetic transport scheme.

Collating the biophysical measurements made in detergent and comparing to other ABC transporter studies, the overall data support a transport mechanism where the binding protein first binds to its substrate in the periplasm to increase the local substrate concentration. The liganded binding protein then associates with the membrane transporter, forming the pre-T state. The opening of the binding protein upon complex formation allows the substrate to be dissociated from the binding protein and to bind to the translocation pathway site of the transporter—this is the outward state. ATP binding and hydrolysis provides energy for the conformational change of the TMDs from outward- to inward-facing and expose the substrate to the cytoplasm. This post hydrolysis ADP- and Pi-bound transporter is the post-T state. There are diverse mechanisms for regulatory inhibition. For MetNI, substrate binding the C-terminal of MetN is believed to stabilize the transporter in its inward-facing conformation, which is a state not poised for either substrate translocation or ATP hydrolysis.

This model describes the MetNI kinetic mechanism. It is predicted that we may borrow knowledge from it to study other members of the ABC Type I transporters. Future challenges include obtaining parallel biophysical measurements of the dif-

ferent conformations in lipid environments to discern artifacts arising from the use of detergents to solubilize MetNI from the membrane bilayer. An important component of the future work includes the establishment of a transport assay setup. There are four main components to understanding the transport cycle: structures of intermediate states, kinetics, ATPase activity, and transport activity. While we have some knowledge on the first three, transport activity of MetNI remains the last major component to be studied.

Chapter 5

APPENDIX

SPR and MST

For inter-molecular binding interaction, which Instrument to try first?

Supposedly the goal is to obtain kinetic and equilibrium properties of an ABC transporter, which technique would you try first? Here we discuss the financial- and time- costs for an experiment for each of the instruments to offer insights and recommendations for starting an experiment. It is recommended one does not start with SPR because first, the gold plated sensor chip is running between $200 to $600 each. Second, the current generation of SPR still requires an extensive amount of time to clean the sensor chip, perform immobilization, and do binding experiment. Besides the time and cost demand, one has pay utmost care when operating SPR. This applies specifically to the docking of a chip that had been used and has been stored in a buffer. The chip has to be cleaned and dried before docking. The cleaning techniques is intricate. We have observed several times when this step was not well practiced, the flow cell was damaged and each flow cell costs about $7000.

ITC can be attempted if there is some knowledge of the what range the affinity falls in. If the expected affinity is in the high nM and low uM, it is feasible to start with ITC. Since the output signal depends entirely on the heat exchange of the binding reaction, it is possible that such heat exchange is so minimal that it is not detectable by ITC, hence the false negatives.

Perturbations

SPR requires immobilization of one of the binding partner to a sensor chip. Such treatment is considered a perturbation to the system. The immobilization must not obscure the binding site. However, in practice, it is difficult to prevent this; hence the false negative can often occur. For example, there is strong evidence that MetNI binds to MetQ in the presence of ATP and EDTA. However, with several immobilization methods (Ni-NTA immobilizing MetNI or antibody immobilization MetNI) do not give positive binding reading. In fact, with the Ni-NTA method, binding was observed initially, then dissocation occurs quickly even though the concentration of the analyte is constant. This is an indication that Ni-NTA does not

hold onto MetNI tightly to enable it to interact with MetQ in a stable platform. This makes sense as Ni-NTA does not form a covalent bond with MetNI. Explorations are needed to find the right immobilization configuration. False positive, which is immobilization that causes enhancements of the binding activity, can arise from immobilization but is less common.

The perturbation or MST is a fluorescence label of one of the binding partner. False positives arise much more frequent than SPR. Also most of the proteins labeling is not specific. Current labeling methods include the labeling of cysteine or lysine. Given how abundant lysine is, label for an MST measurement is often non-specific. For example, we tried labeling MetNI with both lysine and cysteine chemistry. Unfortunately, no binding responses were reported. The reasons can be that the labeling obscures the binding site for MetQ. The labeling of MetQ with cysteine was successful, however. There is only one cysteine in MetQ. Labeling MetQ is a specific addition of a fluorephore.

There is no perturbation of ITC. The response arise from the heat exchange from the binding reaction. If the binding of the two molecules is exothermic, heat is released. If it is endothermic, heat is absorbed. These are intrinsic properties of each binding reaction, and therefore requires no external treatment to enable measurement. In this respect, ITC is superior to the other two techniques.

Detection Range

What determines the detection range is limited by the physical theorems that the instrument is based on. For instance, for SPR, it is limited by the smallest mass that can change the refraction index of the sensor-chip surface as the change of refractive index is the output of the instrument. For instance, SPR cannot detect a small molecule like L-methionine. SPR can detect from low nM to uM. It is not sensitive to low affinity, in the mM range.

MST have different versions of detection range. The NT. pico is specifically designed for detecting high affinities, often for antibody interaction. The NT.115 is designed to detect from nM to mM. Our observations and comments are specifically for NT. 115 as this is the instrument we used for all the studies reported.

ITC has the capacity to detect nM to mM. However, in practice, very high affinity can be difficult to quantify because it might require so small protein concentration as a titration step that it would be close to impossible to do. Low affinity requires

a very large amount of proteins for measurement. Given that ABC transporters are membrane proteins, whose solubility depends on either detergent or proteolyposome, such high concentration of detergent solubilized protein might compromise its activity and stability.

There had been significant difficulties to characterizing the binding sites that pertains to the limits of the biophysical techniques that are available to study this system. The main techniques that have been explored are SPR, MST, and ITC. With SPR, the lower detectable limit is much bigger than the mass of L-methionine, which is 150 Dalton. Therefore, SPR cannot be used to directly to measure affinities of the L-methionine binding sites. A different technique, based on the phenomenon, MicroScale Thermophoresis (MST), allows for steady state measurement of binding interactions. However, while protein-protein interactions have been characterized successfully with this technique, protein-small molecule interactions are difficult to measure, probably due to the smaller change of conformation change and hydration shell upon binding yielding a small, close to background change in signal.

An indirect SPR assay has been developed to address this technical challenge. MetQ was immobilized via a covalent bond to carboxymethylated dextran CM5 sensor-chip within the microfluidic channels for the Biacore system while MetNI was flowing through the volume in the channels. Since L-methionine has an inhibitory effect on the stability of the complex MetNI-MetQ, as L-methionine binds to each binding site on the complex, more complex is destabilized and this change can be detected by SPR. To do this measurement, both proteins MetNI and MetQ are kept a constant concentration, the concentration of L-methionine varies. Binding information of L-methionine can be extrapolated depending on the cooperativity of the binding sites. Here we discuss how the different binding sites were identified, and how the binding affinity for each site was quantified.

BIBLIOGRAPHY

Aittoniemi, J. et al. (2009). "Review. SUR1: a unique ATP-binding cassette protein that functions as an ion channel regulator". In: *Philos Trans R Soc Lond B Biol Sci* 364.1514, pp. 257–67. ISSN: 1471-2970 (Electronic) 0962-8436 (Linking). DOI: 10.1098/rstb.2008.0142. URL: http://www.ncbi.nlm.nih.gov/pubmed/18990670.

Ames, G. F. et al. (1992). "Traffic ATPases: a superfamily of transport proteins operating from Escherichia coli to humans". In: *Adv Enzymol Relat Areas Mol Biol* 65, pp. 1–47. ISSN: 0065-258X (Print) 0065-258X (Linking). URL: http://www.ncbi.nlm.nih.gov/pubmed/1533298.

Austermuhle, M. I. et al. (2004). "Maltose-binding protein is open in the catalytic transition state for ATP hydrolysis during maltose transport". In: *J Biol Chem* 279.27, pp. 28243–50. ISSN: 0021-9258 (Print) 0021-9258 (Linking). DOI: 10.1074/jbc.M403508200. URL: http://www.ncbi.nlm.nih.gov/pubmed/15117946.

Bao, H., K. Dalal, et al. (2015). "Sequential Action of MalE and Maltose Allows Coupling ATP Hydrolysis to Translocation in the MalFGK2 Transporter". In: *J Biol Chem* 290.42, pp. 25452–60. ISSN: 1083-351X (Electronic) 0021-9258 (Linking). DOI: 10.1074/jbc.M115.671826. URL: http://www.ncbi.nlm.nih.gov/pubmed/26338707.

Bao, H. and F. Duong (2012). "Discovery of an auto-regulation mechanism for the maltose ABC transporter MalFGK2". In: *PLoS One* 7.4, e34836. ISSN: 1932-6203 (Electronic) 1932-6203 (Linking). DOI: 10.1371/journal.pone.0034836. URL: http://www.ncbi.nlm.nih.gov/pubmed/22529943.

– (2013). "ATP alone triggers the outward facing conformation of the maltose ATP-binding cassette transporter". In: *J Biol Chem* 288.5, pp. 3439–48. ISSN: 1083-351X (Electronic) 0021-9258 (Linking). DOI: 10.1074/jbc.M112.431932. URL: http://www.ncbi.nlm.nih.gov/pubmed/23243313.

Berntsson, R. P. et al. (2010). "A structural classification of substrate-binding proteins". In: *FEBS Lett* 584.12, pp. 2606–17. ISSN: 1873-3468 (Electronic) 0014-5793 (Linking). DOI: 10.1016/j.febslet.2010.04.043. URL: http://www.ncbi.nlm.nih.gov/pubmed/20412802.

Borths, E. L. et al. (2005). "In vitro functional characterization of BtuCD-F, the Escherichia coli ABC transporter for vitamin B12 uptake". In: *Biochemistry* 44.49, pp. 16301–9. ISSN: 0006-2960 (Print) 0006-2960 (Linking). DOI: 10.1021/bi0513103. URL: http://www.ncbi.nlm.nih.gov/pubmed/16331991.

Bryan, J. et al. (2007). "ABCC8 and ABCC9: ABC transporters that regulate K+ channels". In: *Pflugers Arch* 453.5, pp. 703–18. ISSN: 0031-6768 (Print) 0031-

6768 (Linking). DOI: 10.1007/s00424-006-0116-z. URL: http://www.ncbi.nlm.nih.gov/pubmed/16897043.

Chen, J. et al. (2001). "Trapping the transition state of an ATP-binding cassette transporter: evidence for a concerted mechanism of maltose transport". In: *Proc Natl Acad Sci U S A* 98.4, pp. 1525–30. ISSN: 0027-8424 (Print) 0027-8424 (Linking). DOI: 10.1073/pnas.041542498. URL: http://www.ncbi.nlm.nih.gov/pubmed/11171984.

Chen, S. et al. (2013). "Carbon catabolite repression of the maltose transporter revealed by X-ray crystallography". In: *Nature* 499.7458, pp. 364–8. ISSN: 1476-4687 (Electronic) 0028-0836 (Linking). DOI: 10.1038/nature12232. URL: http://www.ncbi.nlm.nih.gov/pubmed/23770568.

Cui, J., S. Qasim, and A. L. Davidson (2010). "Uncoupling substrate transport from ATP hydrolysis in the Escherichia coli maltose transporter". In: *J Biol Chem* 285.51, pp. 39986–93. ISSN: 1083-351X (Electronic) 0021-9258 (Linking). DOI: 10.1074/jbc.M110.147819. URL: http://www.ncbi.nlm.nih.gov/pubmed/20959448.

Dawson, R. J. P. and K. P. Locher (2006). "Structure of a bacterial multidrug ABC transporter". In: *Nature* 443.7108, pp. 180–185. ISSN: 0028-0836. DOI: 10.1038/nature05155. URL: %3CGo%20to%20ISI%3E://WOS:000240467000039.

Dawson, R. J. and K. P. Locher (2007). "Structure of the multidrug ABC transporter Sav1866 from Staphylococcus aureus in complex with AMP-PNP". In: *FEBS Lett* 581.5, pp. 935–8. ISSN: 0014-5793 (Print) 0014-5793 (Linking). DOI: 10.1016/j.febslet.2007.01.073. URL: http://www.ncbi.nlm.nih.gov/pubmed/17303126.

Dean, M. and T. Annilo (2005). "Evolution of the ATP-binding cassette (ABC) transporter superfamily in vertebrates". In: *Annu Rev Genomics Hum Genet* 6, pp. 123–42. ISSN: 1527-8204 (Print) 1527-8204 (Linking). DOI: 10.1146/annurev.genom.6.080604.162122. URL: http://www.ncbi.nlm.nih.gov/pubmed/16124856.

Dean, M., A. Rzhetsky, and R. Allikmets (2001). "The human ATP-binding cassette (ABC) transporter superfamily". In: *Genome Res* 11.7, pp. 1156–66. ISSN: 1088-9051 (Print) 1088-9051 (Linking). DOI: 10.1101/gr.184901. URL: http://www.ncbi.nlm.nih.gov/pubmed/11435397.

Dill, Ken A. and Sarina Bromberg (2003). *Molecular driving forces : statistical thermodynamics in chemistry and biology*. New York: Garland Science, xx, 666 p. ISBN: 0815320515. URL: Publisher%20description%20http://www.loc.gov/catdir/enhancements/fy0652/2001053202-d.html.

Duhr, S. and D. Braun (2006a). "Thermophoretic depletion follows Boltzmann distribution". In: *Phys Rev Lett* 96.16, p. 168301. ISSN: 0031-9007 (Print) 0031-9007 (Linking). DOI: 10.1103/PhysRevLett.96.168301. URL: http://www.ncbi.nlm.nih.gov/pubmed/16712279.

Duhr, S. and D. Braun (2006b). "Why molecules move along a temperature gradient". In: *Proc Natl Acad Sci U S A* 103.52, pp. 19678–82. ISSN: 0027-8424 (Print) 0027-8424 (Linking). DOI: 10.1073/pnas.0603873103. URL: http://www.ncbi.nlm.nih.gov/pubmed/17164337.

Ferenci, T. et al. (1986). "Substrate specificity of the Escherichia coli maltodextrin transport system and its component proteins". In: *Biochim Biophys Acta* 860.1, pp. 44–50. ISSN: 0006-3002 (Print) 0006-3002 (Linking). URL: http://www.ncbi.nlm.nih.gov/pubmed/3524683.

Goetz, B. A., E. Perozo, and K. P. Locher (2009). "Distinct gate conformations of the ABC transporter BtuCD revealed by electron spin resonance spectroscopy and chemical cross-linking". In: *FEBS Lett* 583.2, pp. 266–70. ISSN: 1873-3468 (Electronic) 0014-5793 (Linking). DOI: 10.1016/j.febslet.2008.12.020. URL: http://www.ncbi.nlm.nih.gov/pubmed/19101549.

Gould, A. D. and B. H. Shilton (2010). "Studies of the maltose transport system reveal a mechanism for coupling ATP hydrolysis to substrate translocation without direct recognition of substrate". In: *J Biol Chem* 285.15, pp. 11290–6. ISSN: 1083-351X (Electronic) 0021-9258 (Linking). DOI: 10.1074/jbc.M109.089078. URL: http://www.ncbi.nlm.nih.gov/pubmed/20147285.

Gouridis, G. et al. (2015). "Conformational dynamics in substrate-binding domains influences transport in the ABC importer GlnPQ". In: *Nat Struct Mol Biol* 22.1, pp. 57–64. ISSN: 1545-9985 (Electronic) 1545-9985 (Linking). DOI: 10.1038/nsmb.2929. URL: https://www.ncbi.nlm.nih.gov/pubmed/25486304.

Heppel, L. A. (1969). "The effect of osmotic shock on release of bacterial proteins and on active transport". In: *J Gen Physiol* 54.1, pp. 95–113. ISSN: 0022-1295 (Print) 0022-1295 (Linking). URL: http://www.ncbi.nlm.nih.gov/pubmed/19873660.

Higgins, C. F. and G. F. Ames (1981). "Two periplasmic transport proteins which interact with a common membrane receptor show extensive homology: complete nucleotide sequences". In: *Proc Natl Acad Sci U S A* 78.10, pp. 6038–42. ISSN: 0027-8424 (Print) 0027-8424 (Linking). URL: https://www.ncbi.nlm.nih.gov/pubmed/6273842.

Higgins, C. F., I. D. Hiles, et al. (1986). "A family of related ATP-binding subunits coupled to many distinct biological processes in bacteria". In: *Nature* 323.6087, pp. 448–50. ISSN: 0028-0836 (Print) 0028-0836 (Linking). DOI: 10.1038/323448a0. URL: http://www.ncbi.nlm.nih.gov/pubmed/3762694.

Hollenstein, K., D. C. Frei, and K. P. Locher (2007). "Structure of an ABC transporter in complex with its binding protein". In: *Nature* 446.7132, pp. 213–6. ISSN: 1476-4687 (Electronic) 0028-0836 (Linking). DOI: 10.1038/nature05626. URL: http://www.ncbi.nlm.nih.gov/pubmed/17322901.

Hvorup, R. N. et al. (2007). “Asymmetry in the structure of the ABC transporter-binding protein complex BtuCD-BtuF”. In: *Science* 317.5843, pp. 1387–90. ISSN: 1095-9203 (Electronic) 0036-8075 (Linking). DOI: 10.1126/science.1145950. URL: http://www.ncbi.nlm.nih.gov/pubmed/17673622.

Jardetzky, O. (1966). “Simple allosteric model for membrane pumps”. In: *Nature* 211.5052, pp. 969–70. ISSN: 0028-0836 (Print) 0028-0836 (Linking). URL: http://www.ncbi.nlm.nih.gov/pubmed/5968307.

Jin, M. S. et al. (2012). “Crystal structure of the multidrug transporter P-glycoprotein from Caenorhabditis elegans”. In: *Nature* 490.7421, pp. 566–9. ISSN: 1476-4687 (Electronic) 0028-0836 (Linking). DOI: 10.1038/nature11448. URL: http://www.ncbi.nlm.nih.gov/pubmed/23000902.

Johnson, E. et al. (2012). “Inward facing conformations of the MetNI methionine ABC transporter: Implications for the mechanism of transinhibition”. In: *Protein Sci* 21.1, pp. 84–96. ISSN: 1469-896X (Electronic) 0961-8368 (Linking). DOI: 10.1002/pro.765. URL: http://www.ncbi.nlm.nih.gov/pubmed/22095702.

Joseph, B. et al. (2011). “Transmembrane gate movements in the type II ATP-binding cassette (ABC) importer BtuCD-F during nucleotide cycle”. In: *J Biol Chem* 286.47, pp. 41008–17. ISSN: 1083-351X (Electronic) 0021-9258 (Linking). DOI: 10.1074/jbc.M111.269472. URL: http://www.ncbi.nlm.nih.gov/pubmed/21953468.

Kadaba, N. S. et al. (2008). “The high-affinity E. coli methionine ABC transporter: structure and allosteric regulation”. In: *Science* 321.5886, pp. 250–3. ISSN: 1095-9203 (Electronic) 0036-8075 (Linking). DOI: 10.1126/science.1157987. URL: http://www.ncbi.nlm.nih.gov/pubmed/18621668.

Kadner, R. J. (1974). “Transport systems for L-methionine in Escherichia coli”. In: *J Bacteriol* 117.1, pp. 232–41. ISSN: 0021-9193 (Print) 0021-9193 (Linking). URL: http://www.ncbi.nlm.nih.gov/pubmed/4587605%20http://jb.asm.org/content/117/1/232.full.pdf.

– (1975). “Regulation of methionine transport activity in Escherichia coli”. In: *J Bacteriol* 122.1, pp. 110–9. ISSN: 0021-9193 (Print) 0021-9193 (Linking). URL: http://www.ncbi.nlm.nih.gov/pubmed/1091617.

– (1977). “Transport and utilization of D-methionine and other methionine sources in Escherichia coli”. In: *J Bacteriol* 129.1, pp. 207–16. ISSN: 0021-9193 (Print) 0021-9193 (Linking). URL: http://www.ncbi.nlm.nih.gov/pubmed/318639.

Kadner, R. J. and W. J. Watson (1974). “Methionine transport in Escherichia coli: physiological and genetic evidence for two uptake systems”. In: *J Bacteriol* 119.2, pp. 401–9. ISSN: 0021-9193 (Print) 0021-9193 (Linking). URL: http://www.ncbi.nlm.nih.gov/pubmed/4604763.

Karpowich, N. et al. (2001). “Crystal structures of the MJ1267 ATP binding cassette reveal an induced-fit effect at the ATPase active site of an ABC transporter”. In: *Structure* 9.7, pp. 571–86. ISSN: 0969-2126 (Print) 0969-2126 (Linking). URL: http://www.ncbi.nlm.nih.gov/pubmed/11470432.

Kellermann, O. and S. Szmelcman (1974). “Active transport of maltose in Escherichia coli K12. Involvement of a "periplasmic" maltose binding protein”. In: *Eur J Biochem* 47.1, pp. 139–49. ISSN: 0014-2956 (Print) 0014-2956 (Linking). URL: http://www.ncbi.nlm.nih.gov/pubmed/4215651.

Khare, D. et al. (2009). “Alternating access in maltose transporter mediated by rigid-body rotations”. In: *Mol Cell* 33.4, pp. 528–36. ISSN: 1097-4164 (Electronic) 1097-2765 (Linking). DOI: 10.1016/j.molcel.2009.01.035. URL: http://www.ncbi.nlm.nih.gov/pubmed/19250913.

Kim, E. et al. (2013). “A single-molecule dissection of ligand binding to a protein with intrinsic dynamics”. In: *Nat Chem Biol* 9.5, pp. 313–8. ISSN: 1552-4469 (Electronic) 1552-4450 (Linking). DOI: 10.1038/nchembio.1213. URL: https://www.ncbi.nlm.nih.gov/pubmed/23502425.

Korkhov, V. M., S. A. Mireku, and K. P. Locher (2012). “Structure of AMP-PNP-bound vitamin B12 transporter BtuCD-F”. In: *Nature* 490.7420, pp. 367–72. ISSN: 1476-4687 (Electronic) 0028-0836 (Linking). DOI: 10.1038/nature11442. URL: http://www.ncbi.nlm.nih.gov/pubmed/23000901.

Lage, H. (2003). “ABC-transporters: implications on drug resistance from microorganisms to human cancers”. In: *Int J Antimicrob Agents* 22.3, pp. 188–99. ISSN: 0924-8579 (Print) 0924-8579 (Linking). URL: http://www.ncbi.nlm.nih.gov/pubmed/13678820.

Lewinson, O. et al. (2010). “A distinct mechanism for the ABC transporter BtuCD-BtuF revealed by the dynamics of complex formation”. In: *Nat Struct Mol Biol* 17.3, pp. 332–8. ISSN: 1545-9985 (Electronic) 1545-9985 (Linking). DOI: 10.1038/nsmb.1770. URL: http://www.ncbi.nlm.nih.gov/pubmed/20173761.

Linton, K. J. and C. F. Higgins (1998). “The Escherichia coli ATP-binding cassette (ABC) proteins”. In: *Mol Microbiol* 28.1, pp. 5–13. ISSN: 0950-382X (Print) 0950-382X (Linking). URL: http://www.ncbi.nlm.nih.gov/pubmed/9593292.

Liu, C. E. et al. (1999). “Both lobes of the soluble receptor of the periplasmic histidine permease, an ABC transporter (traffic ATPase), interact with the membrane-bound complex. Effect of different ligands and consequences for the mechanism of action”. In: *J Biol Chem* 274.2, pp. 739–47. ISSN: 0021-9258 (Print) 0021-9258 (Linking). URL: https://www.ncbi.nlm.nih.gov/pubmed/9873010.

Liu, P. Q. and G. F. Ames (1998). “In vitro disassembly and reassembly of an ABC transporter, the histidine permease”. In: *Proc Natl Acad Sci U S A* 95.7, pp. 3495–500. ISSN: 0027-8424 (Print) 0027-8424 (Linking). URL: http://www.ncbi.nlm.nih.gov/pubmed/9520394.

Liu, P. Q., C. E. Liu, and G. F. Ames (1999). “Modulation of ATPase activity by physical disengagement of the ATP-binding domains of an ABC transporter, the histidine permease”. In: *J Biol Chem* 274.26, pp. 18310–8. ISSN: 0021-9258 (Print) 0021-9258 (Linking). URL: http://www.ncbi.nlm.nih.gov/pubmed/10373434.

Locher, K. P. (2016). “Mechanistic diversity in ATP-binding cassette (ABC) transporters”. In: *Nat Struct Mol Biol* 23.6, pp. 487–93. ISSN: 1545-9985 (Electronic) 1545-9985 (Linking). DOI: 10.1038/nsmb.3216. URL: http://www.ncbi.nlm.nih.gov/pubmed/27273632.

Locher, K. P., A. T. Lee, and D. C. Rees (2002). “The E. coli BtuCD structure: a framework for ABC transporter architecture and mechanism”. In: *Science* 296.5570, pp. 1091–8. ISSN: 1095-9203 (Electronic) 0036-8075 (Linking). DOI: 10.1126/science.1071142. URL: http://www.ncbi.nlm.nih.gov/pubmed/12004122.

Lu, G. et al. (2005). “ATP hydrolysis is required to reset the ATP-binding cassette dimer into the resting-state conformation”. In: *Proc Natl Acad Sci U S A* 102.50, pp. 17969–74. ISSN: 0027-8424 (Print) 0027-8424 (Linking). DOI: 10.1073/pnas.0506039102. URL: http://www.ncbi.nlm.nih.gov/pubmed/16326809.

Mao, B. et al. (1982). “Hinge-bending in L-arabinose-binding protein. The "Venus's-flytrap" model”. In: *J Biol Chem* 257.3, pp. 1131–3. ISSN: 0021-9258 (Print) 0021-9258 (Linking). URL: http://www.ncbi.nlm.nih.gov/pubmed/7035444.

Moitra, K. and M. Dean (2011). “Evolution of ABC transporters by gene duplication and their role in human disease”. In: *Biol Chem* 392.1-2, pp. 29–37. ISSN: 1437-4315 (Electronic) 1431-6730 (Linking). DOI: 10.1515/BC.2011.006. URL: http://www.ncbi.nlm.nih.gov/pubmed/21194360.

Moody, J. E. et al. (2002). “Cooperative, ATP-dependent association of the nucleotide binding cassettes during the catalytic cycle of ATP-binding cassette transporters”. In: *J Biol Chem* 277.24, pp. 21111–4. ISSN: 0021-9258 (Print) 0021-9258 (Linking). DOI: 10.1074/jbc.C200228200. URL: http://www.ncbi.nlm.nih.gov/pubmed/11964392.

Nguyen, P. T. et al. (2015). “The contribution of methionine to the stability of the Escherichia coli MetNIQ ABC transporter-substrate binding protein complex”. In: *Biol Chem* 396.9-10, pp. 1127–34. ISSN: 1437-4315 (Electronic) 1431-6730 (Linking). DOI: 10.1515/hsz-2015-0131. URL: http://www.ncbi.nlm.nih.gov/pubmed/25803078.

Oldham, M. L. and J. Chen (2011a). “Crystal structure of the maltose transporter in a pretranslocation intermediate state”. In: *Science* 332.6034, pp. 1202–5. ISSN: 1095-9203 (Electronic) 0036-8075 (Linking). DOI: 10.1126/science.1200767. URL: http://www.ncbi.nlm.nih.gov/pubmed/21566157.

Oldham, M. L. and J. Chen (2011b). "Snapshots of the maltose transporter during ATP hydrolysis". In: *Proc Natl Acad Sci U S A* 108.37, pp. 15152–6. ISSN: 1091-6490 (Electronic) 0027-8424 (Linking). DOI: 10.1073/pnas.1108858108. URL: http://www.ncbi.nlm.nih.gov/pubmed/21825153.

Oldham, M. L., S. Chen, and J. Chen (2013). "Structural basis for substrate specificity in the Escherichia coli maltose transport system". In: *Proc Natl Acad Sci U S A* 110.45, pp. 18132–7. ISSN: 1091-6490 (Electronic) 0027-8424 (Linking). DOI: 10.1073/pnas.1311407110. URL: https://www.ncbi.nlm.nih.gov/pubmed/24145421.

Oldham, M. L., D. Khare, et al. (2007). "Crystal structure of a catalytic intermediate of the maltose transporter". In: *Nature* 450.7169, pp. 515–21. ISSN: 1476-4687 (Electronic) 0028-0836 (Linking). DOI: 10.1038/nature06264. URL: http://www.ncbi.nlm.nih.gov/pubmed/18033289.

Orelle, C., F. J. Alvarez, et al. (2010). "Dynamics of alpha-helical subdomain rotation in the intact maltose ATP-binding cassette transporter". In: *Proc Natl Acad Sci U S A* 107.47, pp. 20293–8. ISSN: 1091-6490 (Electronic) 0027-8424 (Linking). DOI: 10.1073/pnas.1006544107. URL: http://www.ncbi.nlm.nih.gov/pubmed/21059948.

Orelle, C., T. Ayvaz, et al. (2008). "Both maltose-binding protein and ATP are required for nucleotide-binding domain closure in the intact maltose ABC transporter". In: *Proc Natl Acad Sci U S A* 105.35, pp. 12837–42. ISSN: 1091-6490 (Electronic) 0027-8424 (Linking). DOI: 10.1073/pnas.0803799105. URL: http://www.ncbi.nlm.nih.gov/pubmed/18725638.

Pinkett, H. W. et al. (2007). "An inward-facing conformation of a putative metal-chelate-type ABC transporter". In: *Science* 315.5810, pp. 373–7. ISSN: 1095-9203 (Electronic) 0036-8075 (Linking). DOI: 10.1126/science.1133488. URL: http://www.ncbi.nlm.nih.gov/pubmed/17158291.

Piperno, J. R. and D. L. Oxender (1968). "Amino acid transport systems in Escherichia coli K-12". In: *J Biol Chem* 243.22, pp. 5914–20. ISSN: 0021-9258 (Print) 0021-9258 (Linking). URL: http://www.ncbi.nlm.nih.gov/pubmed/4880290.

Quiocho, F. A. (1990). "Atomic structures of periplasmic binding proteins and the high-affinity active transport systems in bacteria". In: *Philos Trans R Soc Lond B Biol Sci* 326.1236, pp. 341–51, 341–51. ISSN: 0962-8436 (Print) 0962-8436 (Linking). URL: http://www.ncbi.nlm.nih.gov/pubmed/1970641.

Rees, D. C., E. Johnson, and O. Lewinson (2009). "ABC transporters: the power to change". In: *Nat Rev Mol Cell Biol* 10.3, pp. 218–27. ISSN: 1471-0080 (Electronic) 1471-0072 (Linking). DOI: 10.1038/nrm2646. URL: http://www.ncbi.nlm.nih.gov/pubmed/19234479.

Riordan, J. R. (2008). "CFTR function and prospects for therapy". In: *Annu Rev Biochem* 77, pp. 701–26. ISSN: 0066-4154 (Print) 0066-4154 (Linking). DOI: 10.1146/annurev.biochem.75.103004.142532. URL: http://www.ncbi.nlm.nih.gov/pubmed/18304008.

Schmitt, L. et al. (2003). "Crystal structure of the nucleotide-binding domain of the ABC-transporter haemolysin B: identification of a variable region within ABC helical domains". In: *J Mol Biol* 330.2, pp. 333–42. ISSN: 0022-2836 (Print) 0022-2836 (Linking). URL: http://www.ncbi.nlm.nih.gov/pubmed/12823972.

Sharff, A. J. et al. (1992). "Crystallographic evidence of a large ligand-induced hinge-twist motion between the two domains of the maltodextrin binding protein involved in active transport and chemotaxis". In: *Biochemistry* 31.44, pp. 10657–63. ISSN: 0006-2960 (Print) 0006-2960 (Linking). URL: http://www.ncbi.nlm.nih.gov/pubmed/1420181.

Sharma, S. and A. L. Davidson (2000). "Vanadate-induced trapping of nucleotides by purified maltose transport complex requires ATP hydrolysis". In: *J Bacteriol* 182.23, pp. 6570–6. ISSN: 0021-9193 (Print) 0021-9193 (Linking). URL: http://www.ncbi.nlm.nih.gov/pubmed/11073897.

Spurlino, J. C., G. Y. Lu, and F. A. Quiocho (1991). "The 2.3-A resolution structure of the maltose- or maltodextrin-binding protein, a primary receptor of bacterial active transport and chemotaxis". In: *J Biol Chem* 266.8, pp. 5202–19. ISSN: 0021-9258 (Print) 0021-9258 (Linking). URL: https://www.ncbi.nlm.nih.gov/pubmed/2002054.

Tomatsu, H. et al. (2007). "An Arabidopsis thaliana high-affinity molybdate transporter required for efficient uptake of molybdate from soil". In: *Proc Natl Acad Sci U S A* 104.47, pp. 18807–12. ISSN: 1091-6490 (Electronic) 0027-8424 (Linking). DOI: 10.1073/pnas.0706373104. URL: http://www.ncbi.nlm.nih.gov/pubmed/18003916.

Treptow, N. A. and H. A. Shuman (1985). "Genetic evidence for substrate and periplasmic-binding-protein recognition by the MalF and MalG proteins, cytoplasmic membrane components of the Escherichia coli maltose transport system". In: *J Bacteriol* 163.2, pp. 654–60. ISSN: 0021-9193 (Print) 0021-9193 (Linking). URL: http://www.ncbi.nlm.nih.gov/pubmed/3894331.

Vigonsky, E., E. Ovcharenko, and O. Lewinson (2013). "Two molybdate/tungstate ABC transporters that interact very differently with their substrate binding proteins". In: *Proc Natl Acad Sci U S A* 110.14, pp. 5440–5. ISSN: 1091-6490 (Electronic) 0027-8424 (Linking). DOI: 10.1073/pnas.1213598110. URL: http://www.ncbi.nlm.nih.gov/pubmed/23513215.

Yang, J. G. and D. C. Rees (2015). "The allosteric regulatory mechanism of the Escherichia coli MetNI methionine ATP binding cassette (ABC) transporter". In: *J Biol Chem* 290.14, pp. 9135–40. ISSN: 1083-351X (Electronic) 0021-9258

(Linking). DOI: 10.1074/jbc.M114.603365. URL: http://www.ncbi.nlm.nih.gov/pubmed/25678706.

Yu, J. et al. (2015). "Structural basis for substrate specificity of an amino acid ABC transporter". In: *Proc Natl Acad Sci U S A* 112.16, pp. 5243–8. ISSN: 1091-6490 (Electronic) 0027-8424 (Linking). DOI: 10.1073/pnas.1415037112. URL: https://www.ncbi.nlm.nih.gov/pubmed/25848002.